Neuropharmacology 209 (2022) 109020

Contents lists available at ScienceDirect

Neuropharmacology

journal homepage: www.elsevier.com/locate/neuropharm

In vitro and in vivo pharmaco-dynamic study of the novel fentanyl derivatives: Acrylfentanyl, Ocfentanyl and Furanylfentanyl

Sabrine Bilel [a], Joaquim Azevedo Neto [b], Raffaella Arfè [a], Micaela Tirri [a], Rosa Maria Gaudio [a,c], Anna Fantinati [d], Tatiana Bernardi [d], Federica Boccuto [d], Beatrice Marchetti [a], Giorgia Corli [a], Giovanni Serpelloni [e], Fabio De-Giorgio [f,g], Davide Malfacini [h], Claudio Trapella [d], Girolamo Calo' [h], Matteo Marti [a,c,i,*]

[a] Department of Translational Medicine, Section of Legal Medicine and LTTA Centre, University of Ferrara, Italy
[b] Department of Neuroscience and Rehabilitation, Section of Pharmacology, University of Ferrara, Via Fossato di Mortara 17/19, 44121, Ferrara, Italy
[c] Center of Gender Medicine, University of Ferrara, Italy
[d] Department of Chemistry and Pharmaceutical Sciences, University of Ferrara, Italy
[e] Neuroscience Clinical Center & TMS Unit Verona, Italy and Department of Psychiatry in the College of Medicine, Drug Policy Institute, University of Florida, Gainesville, FL, United States
[f] Institute of Public Health, Section of Legal Medicine, Università Cattolica Del Sacro Cuore, Roma, Italy
[g] Fondazione Policlinico Universitario A. Gemelli IRCCS, Roma, Italy
[h] Department of Pharmaceutical and Pharmacological Sciences, University of Padua, Italy
[i] Collaborative Center of the National Early Warning System, Department for Anti-Drug Policies, Presidency of the Council of Ministers, Italy

ARTICLE INFO

Keywords:
Fentanyl
Acrylfentanyl
Furanylfentanyl
Ocfentanyl
Novel psychoactive substances mu opioid receptor
β-arrestin 2
Naloxone
Cardiorespiratory changes
Analgesia

ABSTRACT

Fentanyl derivatives (FENS) belongs to the class of Novel Synthetic Opioids that emerged in the illegal drug market of New Psychoactive Substances (NPS). These substances have been implicated in many cases of intoxication and death with overdose worldwide. Therefore, the aim of this study is to investigate the pharmaco-dynamic profiles of three fentanyl (FENT) analogues: Acrylfentanyl (ACRYLF), Ocfentanyl (OCF) and Furanylfentanyl (FUF). In vitro, we measured FENS opioid receptor efficacy, potency, and selectivity in calcium mobilization studies performed in cells coexpressing opioid receptors and chimeric G proteins and their capability to promote the interaction of the mu receptor with G protein and β-arrestin 2 in bioluminescence resonance energy transfer (BRET) studies. In vivo, we investigated the acute effects of the systemic administration of ACRYLF, OCF and FUF (0.01–15 mg/kg i.p.) on mechanical and thermal analgesia, motor impairment, grip strength and cardiorespiratory changes in CD-1 male mice. Opioid receptor specificity was investigated in vivo using naloxone (NLX; 6 mg/kg i.p) pre-treatment. In vitro, the three FENS were able to activate the mu opioid receptor in a concentration dependent manner with following rank order potency: FUF > FENT=OCF > ACRYLF. All compounds were able to elicit maximal effects similar to that of dermorphin, with the exception of FUF which displayed lower maximal effects thus behaving as a partial agonist. In the BRET G-protein assay, all compounds behaved as partial agonists for the β-arrestin 2 pathway in comparison with dermorphin, whereas FUF did not promote β-arrestin 2 recruitment, behaving as an antagonist. In vivo, all the compounds increased mechanical and thermal analgesia with following rank order potency ACRYLF = FENT > FUF > OCF and impaired motor and cardiorespiratory parameters. Among the substances tested, FUF showed lower potency for cardiorespiratory and motor effects. These findings reveal the risks associated with the use of FENS and the importance of studying the pharmaco-dynamic properties of these drugs to better understand possible therapeutic interventions in the case of toxicity.

* Corresponding author. Department of Translational Medicine, Section of Legal Medicine, University of Ferrara, via Fossato di Mortara 70, 44121, Ferrara, Italy.
E-mail address: matteo.marti@unife.it (M. Marti).

https://doi.org/10.1016/j.neuropharm.2022.109020
Received 9 July 2021; Received in revised form 16 February 2022; Accepted 24 February 2022
Available online 2 March 2022

Abbreviations

NSO	Novel Synthetic Opioids
FENS	Fentanyl derivatives
FENT	Fentanyl; N-(1-(2- feniletil)-4- piperidinil)-N- fenil-propanammide
ACRYLF	Acrylfentanyl; N-Phenyl-N-[1-(2-phenylethyl) piperidin-4-yl]prop-2-enamide
FUF	Furanylfentanyl; N-Phenyl-N-[1-(2-phenylethyl) piperidin-4-yl]furan-2-carboxamide
OCF	Ocfentanyl; N-(2-Fluorophenyl)-2-methoxy-N-[1-(2-phenylethyl) piperidin-4-yl]acetamide
NLX	Naloxone; (4R,4aS,7aR,12bS)-4a,9-dihydroxy-3-prop-2-enyl-2,4,5,6,7a,13-hexahydro-1H-4,12methanobenzofuro[3,2e]isoquinolin-7-one
BRET	Bioluminescence Resonance Energy Transfer assay

1. Introduction

Novel Synthetic Opioids (NSO) are a growing class of new psychoactive substances (NPS) mostly consisting of analogues of fentanyl (FENT) linked to numerous overdose and fatalities worldwide. NSO accounted for just 2% of NPS identified in 2014; this rose to 9% by 2018 (United Nations Office on Drugs and Crime UNDOC, 2020). Overall, 49 NSOs have been detected on Europe's drug market since 2009 (EMCDDA, 2019), including FENT, its analogues used in medical therapy (e.g. Sufentanyl, Alfentanyl and Remifentanyl; Lemmens, 1995), novel non-pharmaceutical FENT derivatives (e.g. Ocfentanyl, Furanylfentanyl, Acetylfentanyl, Carfentanyl, Acrylfentanyl, Tetrahydrofuranylfentanyl, etc.) and other molecules. FENS recently seized as NSOs are usually generated by replacement of the ethylphenyl moiety (Isofentanyl, β-hydroxythiofentanyl) or modification of FENT propionyl chain (Acrylfentanyl (ACRYLF), Ocfentanyl (OCF), Acetylfentanyl, Furanylfentanyl (FUF), Butyrylfentanyl and Isobutyrylfentanyl). An estimated 58 million people used opioids in 2018, this number is considered lower in respect to cannabis users (192 millions). However, the number of deaths reflects the toxicity of opioids. Yet, opioid use has been involved in 66% of the estimated 167,000 deaths related to drug use disorders in 2017. FENT is a synthetic opioid agonist with analgesic and anaesthetic properties and is approximately 100 times more potent than morphine. New FENS are structurally similar to FENT and therefore often have comparable biological effects (Solimini et al., 2018). The severe adverse effects of FENS include euphoria, drowsiness, dizziness, confusion, miosis, nausea, vomiting, confusion, constipation, sedation, skin rash, respiratory depression, unconsciousness, coma, and death. In 2018, synthetic FENS were implicated in two thirds of the 67,367 overdose deaths registered in the United States. Similar findings have been also reported in Canada, Australia and Europe, but with lower numbers. Novel FENS are frequently sold as heroin adulterant. The overdose death related to these substances is mainly driven by the unpredictability of their potency. Moreover, in some deaths related to FENS such as ACRYLF, OCF and FUF (Fig. 1), no heroin was found. The high availability, the low price and the high potency of these compounds could explain the trends of their abuse. ACRYLF was first developed as an analogue of FENT in 1981 (Zhu et al., 1981). It is an acrylamide derivative of 4-anilinopiperidine and is an unsaturated analogue of FENT. In the last few years it has appeared online as a research chemical. In 2016, the European Monitoring Centre for Drugs and Drug Addiction (EMCDDA) has reported a total of 130 deaths caused by ACRYLF in United States and Europe (EMCDDA, 2016). OCF had been studied clinically for its analgesic activity during the early 1990s (Huang et al., 1986). It was found to have a relative potency 200 times greater than that of morphine and it is more potent than FENT with fewer adverse effects, regarding respiratory depression and bradycardia (Huang et al., 1986). OCF is among the 14 FENT derivatives that have been reported in Europe within 2012–2016. It has been associated with some intoxication cases and deaths in Belgium and Switzerland (Zwaliska, 2017). FUF is a FENT derivative that differs from FENT in that it has a furanyl ring in place of the methyl group adjacent to the carbonyl bridge. The first report of a FUF-related intoxication was recorded in 2015 in the USA. In 2016, a total of 494 forensic cases of FUF, including 128 confirmed fatalities, were reported to the DEA. In 2017, the EMCDDA reported a total of 29 serious adverse events (10 acute intoxications and 19 deaths) associated with FUF in Estonia, Germany, United Kingdom, Sweden and Norway (EMCDDA, 2017). Data on the pharmacology of these compounds are limited. Therefore, the aim of this study was to investigate the pharmaco-dynamic profile of the ACRYLF, OCF and FUF compared with FENT. To evaluate the in vitro basic pharmacological profile of these compounds, a calcium mobilization assay was performed using cells expressing opioid receptors and chimeric G-proteins (Camarda and Calo', 2013). Moreover, a bioluminescence resonance energy transfer (BRET) assay was also used to investigate the ability of the compounds to promote mu receptor interaction with G-protein and β-arrestin 2 (Molinari et al., 2010). We investigated the acute effects of the three

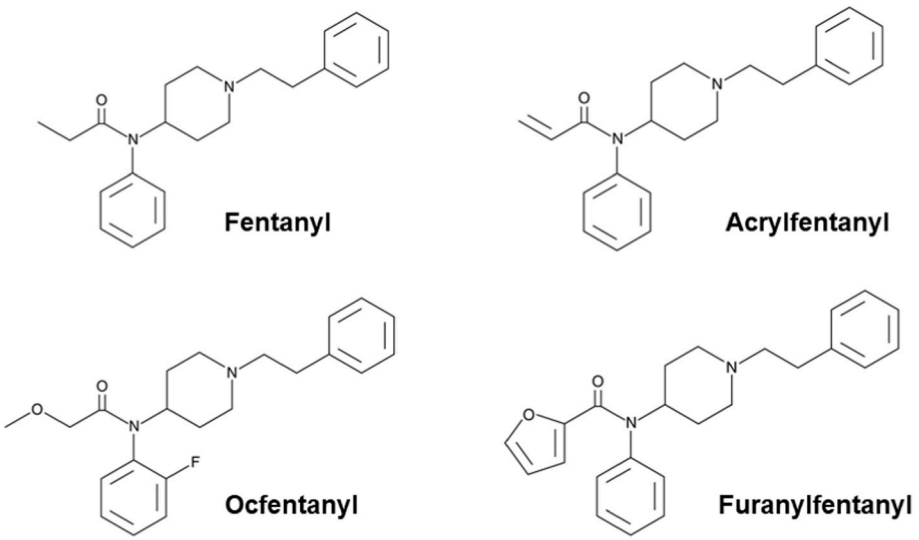

Fig. 1. Chemical structures of Fentanyl; Acrylfentanyl; Ocfentanyl and Furanylfentanyl.

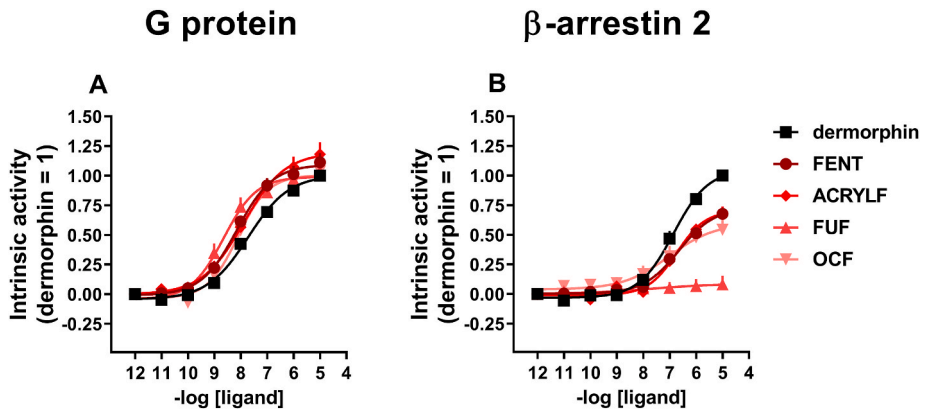

Fig. 2. BRET assay. Concentration response curve to dermorphin, FENT, ACRYLF, FUF, and OCF for mu/G protein (panel A) and mu/β-arrestin 2 (panel B) interaction. Data are the mean ± s.e.m. of 5 separate experiments made in duplicate.

FENS in comparison to FENT, in vivo, on acute mechanical and thermal analgesia, motor impairment, muscle strength and cardiorespiratory changes (heart rate, respiratory rate, SpO_2 saturation and pulse distention) in CD-1 male mice. Opioid receptor specificity was investigated in vivo using NLX pre-treatment in all the tests.

2. Materials and methods

2.1. In vitro studies

2.1.1. Drugs and reagents

All cell culture media and supplements were from Invitrogen (Thermo Fisher Scientific Inc. MA, USA). Dermorphin, DPDPE, and Dynorphin A were synthetized in the laboratory of Prof Remo Guerrini (University of Ferrara). FENT was from Bio-Techne (UK) (authorization SP/168 November 04, 2019 to MM). The FENT derivatives, ACRYLF, OCF and FUF were purchased from LGC standards (LGC Standards S.r.l., Sesto San Giovanni, Milan, Italy) (authorization SP/168 November 04, 2019 to MM) while naloxone was purchased from Sigma Aldrich (St. Louis, MO, USA). Opioid peptides were solubilized in bidistilled water, whereas all other compounds were solubilized in DMSO at a final concentration of 10 mM. Stock solutions of ligands were stored at −20 °C. Serial dilutions were made in each assay buffer.

2.1.2. Calcium mobilization assay

CHO cells stably coexpressing the human recombinant mu or kappa receptors with the C-terminally modified $G\alpha_{qi5}$ and CHO cells coexpressing the delta receptor and the $G\alpha_{qG66Di5}$ chimeric protein were generated as previously described (Camarda and Calo, 2013). Cells were cultured in medium consisting of Dulbecco's modified Eagle's medium (DMEM)/HAMS F12 (1:1) supplemented with 10% fetal bovine serum (FBS), penicillin (100 IU/ml), streptomycin (100 mg/ml), geneticin (G418; 200 μg/ml) and hygromycin B (100 μg/ml). Cell cultures were kept at 37 °C in 5% CO_2/humidified air. When confluence was reached (3–4 days), cells were sub-cultured as required using trypsin/EDTA and used for experimentation. Cells were seeded at a density of 50,000 cells/well into 96-well black, clear-bottom plates. After 24 h incubation the cells were incubated with Hank's Balanced Salt Solution (HBSS) supplemented with 2.5 mM probenecid, 3 μM of the calcium sensitive fluorescent dye Fluo-4 AM, 0.01% pluronic acid and 20 mM HEPES (pH 7.4) for 30 min at 37 °C. Afterwards the loading solution was aspirated followed by a washing step with 100 μl/well of HBSS, HEPES (20 mM, pH 7.4), 2.5 mM probenecid and 500 μM Brilliant Black. Subsequently 100 μl/well of the same buffer was added. After placing cell culture and compound plates into the FlexStation II (Molecular Devices, Sunnyvale, CA, USA), the changes in fluorescence of the cell-loaded calcium sensitive dye Fluor-4 AM were measured.

2.1.3. BRET assay

SH-SY5Y Cells stably co-expressing the different pairs of fusion proteins i.e. mu-RLuc/Gβ1-RGFP and mu-RLuc/β-arrestin 2-RGFP were prepared using a pantropic retroviral expression system as described previously (Molinari et al., 2010; Malfacini et al., 2015). Cells were grown in Dulbecco's modified Eagle's medium (DMEM)/HAMS F12 (1:1) supplemented with 10% fetal bovine serum, penicillin G (100 units/ml), streptomycin (100 μg/ml), L-glutamine (2 mM), fungizone (1 μg/ml), geneticin (G418; 400 μg/ml) and hygromycin B (100 μg/ml) in a humidified atmosphere of 5% CO_2 at 37 °C. For G-protein experiments, enriched plasma membrane aliquots from mu-RLuc/Gβ1-RGFP cells were prepared by differential centrifugation; cells were detached with PBS/EDTA solution (1 mM, pH 7.4 NaOH) then, after 5 min 500 g centrifugation, Dounce-homogenized (30 strokes) in cold homogenization buffer (TRIS 5 mM, EGTA 1 mM, DTT 1 mM, pH 7.4 HCl) in the presence of sucrose (0.32 M). Three following centrifugation steps were performed at 10 min 1000 g (4 °C) and the supernatants kept. Two 20 min 24,000 g (4 °C) subsequent centrifugation steps (the second in the absence of sucrose) were performed for separating enriched membranes that after discarding the supernatant were kept in ultrapure water at −80 °C (Vachon et al., 1987). Membrane protein was determined using the QPRO-BCA kit (Cyanagen Srl, Bologna, IT) and the multimode Ensight plate reader (Perkin Elmer, Waltham, US). Luminescence in membranes and cells was recorded in 96-well white opaque microplates (Perkin Elmer, Waltham, MA, USA) using the Victor 2030 luminometer (PerkinElmer, Waltham, MA, USA). For the determination of receptor/G-protein interaction, membranes (3 μg of protein) prepared from cells co-expressing mu-RLuc/Gβ1-RGFP were added to wells in Dulbecco's phosphate-buffered saline(DPBS). For the determination of receptor/β-arrestin 2 interaction, whole cells co-expressing mu-RLuc/β-arrestin 2-RGFP were plated 24 h before the experiment (100,000 cells/well). The cells were prepared for the experiment by substituting the medium with PBS with $MgCl_2$ (0.5 mM) and $CaCl_2$ (0.9 mM). Coelenterazine at a final concentration of 5 μM was injected 15 min prior reading the cell plate. Different concentrations of ligands in 20 μL of PBS - BSA 0.01% were added and incubated 5 min before reading luminescence. All experiments were performed at room temperature.

2.1.4. Data analysis and terminology

Pharmacological terminology adopted in this report is consistent with IUPHAR recommendations (Neubig et al., 2003). All data are expressed as the mean ± standard error of the mean (s.e.m.) of *n* experiments. For potency values 95% confidence limits ($CL_{95\%}$) were indicated. In calcium mobilization studies, agonist effects were expressed as maximum change in percent over the baseline fluorescence. Baseline fluorescence was measured in wells treated with saline. In BRET studies agonist effects were calculated as BRET ratio between CPS

measured for the RGFP and RLuc light emitted using 510(10) and 460 (25) filters (PerkinElmer, Waltham, MA, USA), respectively. Maximal agonist effects were expressed as fraction of the dermorphin maximal effects which was determined in every assay plate (dermorphin = 1). Concentration response curve to agonists were fitted with the four parameter logistic nonlinear regression model:

$$\text{Effect} = \text{Baseline} + \frac{(E_{max} - \text{Baseline})}{(1 + 10^{(LogEC_{50} - Log_{[compound]})Hillslope})}$$

For all assays, agonist potencies are given as pEC_{50} i.e. the negative logarithm to base 10 of the molar concentration of an agonist that produces 50% of the maximal effect of that agonist. The potency of antagonists was expressed as pA_2 derived from the following equation: $pA_2 = -\log[(CR-1)/[A]]$, assuming a slope value equal to unity, where CR indicates the ratio between agonist potency in the presence and absence of antagonist and [A] is the molar concentration of the antagonist (Kenakin, 2004).

2.2. In vivo studies

2.2.1. Animals

Four hundred thirty-two Male ICR (CD-1®) mice weighing 30–35 g (Centralized Preclinical Research Laboratory, University of Ferrara, Italy) were group housed (5 mice per cage; floor area per animal was 80 cm^2; minimum enclosure height was 12 cm), exposed to a 12:12-h light-dark cycle (light period from 6:30 a.m. to 6:30 p.m.) at a temperature of 20–22 °C and humidity of 45–55% and were provided ad libitum access to food (Diet 4RF25 GLP; Mucedola, Settimo Milanese, Milan, Italy) and water. The experimental protocols performed in the present study were in accordance with the U.K. Animals (Scientific Procedures) Act of 1986 and associated guidelines and the new European Communities Council Directive of September 2010 (2010/63/EU). Experimental protocols were approved by the Italian Ministry of Health (license n. 335/2016-PR) and by the Animal Welfare Body of the University of Ferrara. According to the ARRIVE guidelines, all possible efforts were made to minimise the number of animals used, to minimise the animals' pain and discomfort.

2.2.2. Drug preparation and dose selection

Drugs were dissolved in saline solution (0.9% NaCl) that was also used as the vehicle. The opioid receptor antagonist NLX (6 mg/kg) was administered 15 min before FENT, ACRYLF, OCF and FUF injections. The dose of 6 mg/kg of NLX was used in our previous study (Bilel et al., 2020) and proved its efficacy in blocking the actions of morphine without having any effect per se. Higher doses of NLX (> 6 mg/kg) were tested in our preliminary data. In particular, the dose of 10 mg/kg induced sensorimotor alterations, increased slightly analgesia and also increased heart and breath rates in our animal model. Indeed, the dose of 6 mg/kg is selected for this study.The protocol set in the present study for naloxone injections is aimed to mimic clinical evidence: in fact, it has been reported the need of naloxone redosing to revert fentanyl's toxicity (in particular respiratory depression; Klebacher et al., 2017; Rzasa Lynn and Galinkin, 2018). Thus, a second full dose of naloxone (6 mg/kg) was injected 55 min after the first one in order to better antagonize FENS effects and counteract their reappearance. Drugs were administered by intraperitoneal (i.p.) injection at a volume of 4 μl/g. The range of doses of FENS tested (0.01–15 mg/kg i.p.) was chosen based on our previous studies (Bilel et al., 2019; Bilel et al., 2020).

2.2.3. Behavioural studies

The effects of the four FENS were investigated using a battery of behavioural tests widely used in pharmacology safety studies for the preclinical characterization of new psychoactive substances in rodents (Vigolo et al., 2015; Ossato et al., 2015; Canazza et al., 2016; Fantinati et al., 2017; Ossato et al., 2018; Marti et al., 2019; Bilel et al., 2020; Bilel et al., 2021). All experiments were performed between 8:30 a.m. and 2:00 p.m. Experiments were conducted blindly by trained observers working in pairs (Ossato et al., 2016). Mouse behaviour (motor responses) was videotaped and analysed offline by a different trained operator who gives test scores.

2.2.3.1. Evaluation of pain induced by a mechanical and a thermal stimulus. *Acute mechanical nociception* was evaluated using the tail pinch test (Vigolo et al., 2015). A special rigid probe connected to a digital dynamometer (ZP-50N, IMADA, Japan) was gently placed on the tail of the mouse (in the distal portion), and progressive pressure was applied. When the mouse flicked its tail, the pressure was stopped and the digital instrument recorded the maximum peak of weight supported (g/force). A cut off (500 g/force) was set to avoid tissue damage. The test was repeated three times and the final value was calculated by averaging the three obtained scores. *Acute thermal nociception* was evaluated using the tail withdrawal test (Vigolo et al., 2015). The mouse was restrained in a dark plastic cylinder and half of its tail was dipped in 48 °C water, Then, the length of time (in s) the tail was left in the water was recorded. A cut off (15 s) was set to avoid tissue damage. Acute mechanical and thermal nociception was measured at 0, 35, 55, 90, 145, 205, 265 and 325 min post injection.

2.2.3.2. Motor activity assessment. Alterations of motor activity induced by FENS were measured using the drag and the accelerod tests (Bilel et al., 2020). In the *drag test*, the mouse was lifted by the tail, leaving the front paws on the table, and was dragged backward at a constant speed of about 20 cm/s for a fixed distance (100 cm). The number of steps performed by each paw was recorded by two different observers. For each animal, five to seven measurements were collected. The drag test was performed at 0, 45, 70, 105, 160, 220, 280 and 340 min post injection. In the *accelerod test*, the animals were placed on a rotating cylinder that automatically increases in velocity in a constant manner (0–60 rotations/min in 5 min). The time spent on the cylinder was measured. The accelerod test was performed at 0, 40, 60, 95, 150, 210, 270 and 330 min post injection.

2.2.3.3. Evaluation of skeletal muscle strength (grip strength). This test was used to evaluate the skeletal muscle strength of the mice (Bilel et al., 2020).The grip-strength apparatus (ZP-50N, IMADA) is comprised of a wire grid (5 × 5 cm) connected to an isometric force transducer (dynamometer). In the grip-strength test, mice were held by their tails and allowed to grasp the grid with their forepaws. The mice were then gently pulled backward by the tail until the grid was released. The average force exerted by each mouse before losing its grip was recorded. The mean of three measurements for each animal was calculated, and the mean average force was determined. The skeletal muscle strength is expressed in gram force (gf) and was recorded and processed using IMADA ZP-Recorder software. The grip strength was measured at 0, 15, 35, 70, 125, 185, 245 and 305 min post injection.

2.2.3.4. Cardiorespiratory analysis. The experimental protocol to detect the cardiorespiratory parameters used in this study is designed to monitor awake and freely moving animals with no invasive instruments and with minimal handling (Bilel et al., 2020). A collar was placed around the neck of the animal; this collar has a sensor that continuously detects heart rate, respiratory rate, oxygen saturation and pulse distention with a frequency of 15 Hz. While running the experiment, the mouse moves freely in the cage (with no access to food and water) monitored by the sensor collar using the software MouseOx Plus (STARR Life Sciences® Corp. Oakmont, PA). In the first hour, a collar was placed around the animal's neck to simulate the real one used in the test, thus minimising the possible effects of stress during the experiment. The real collar (with sensor) was then substituted, and baseline parameters were monitored for 60 min. Subsequently, the mice were given FENT,

ACRYLF, OCF and FUF by i.p. injection, and data was recorded for 5 h.

2.2.4. Data and statistical analysis

Antinociceptive effects (tail withdrawal and tail pinch tests) are calculated as the percent of maximal possible effect {EMax% = [(test - control latency)/(cut off time - control)] X 100}. Tail withdrawal and tail pinch are expressed as Emax %. Drag and accelerod are expressed in percentage of basal value (%), maximal muscle strength is expressed as gf, heart rate is expressed as heart beats per min (bpm), pulse distention (vessel diameter changes) is expressed as μm, respiratory rate is expressed as respiratory rate per minute (rrpm) and SpO_2 saturation (oxygen blood saturation) is expressed as %.

Statistical analysis of the effects of the substances at different doses over time and of antagonism were performed using a two-way ANOVA followed by a Bonferroni test for multiple comparisons. Statistical analysis was performed using Prism software (GraphPad Prism, USA).

The mean effect values represent the average of the effects induced by each compound at each dose over the time course of the experiment. For Tail pinch, Tail withdrawal, accelerod, drag and grip strength tests, the mean effects were calculated for the 5 h time-course (Figs. 3–7; Panels C and D). However, for the cardiorespiratory curves (Figs. 8–11; Panels C and D), the mean effect values were calculated for the first 2 h of measurements, since after this time point the effects of the drugs disappeared.

The ED_{50} values were calculated (where it was possible) using nonlinear regression which presents the best fit values of log dose of agonist vs. response (GraphPad Prism).

3. Results

3.1. In vitro studies

3.1.1. Calcium mobilization studies

In CHO cells stably transfected with the human mu opioid receptor, the standard agonist dermorphin evoked a robust concentration-dependent stimulation of calcium release displaying high potency (pEC_{50} of 8.19) and maximal effects (319 ± 13% over the basal values). FENT mimicked the stimulatory effect elicited by dermorphin showing similar potency and maximal effects. All FENT derivatives were able to activate the mu opioid receptor in a concentration dependent manner with the following rank order potency: FENT = ACRYLF ≥ FUF = OCF. Regarding ligand efficacy, all compounds were able to elicit maximal effects similar to that of dermorphin, with the exception of FUF that displayed statistically significantly lower maximal effects thus behaving as a partial agonist (Table 1).

In CHO_{delta} cells, the standard agonist DPDPE evoked a robust concentration-dependent stimulation of calcium release with high potency (pEC_{50} of 7.47) and maximal effects (230 ± 18% over the basal values). All other compounds were either inactive or displayed an incomplete concentration response curve, stimulating calcium mobilization only at micromolar concentrations.

In CHO_{kappa} cells, the standard agonist dynorphin A evoked a robust concentration-dependent stimulation of calcium release with very high potency (pEC_{50} of 8.81) and maximal effects (257 ± 34% over the basal values). All other compounds were either inactive or displayed an incomplete concentration response curve, stimulating calcium mobilization only at micromolar concentrations.

3.1.2. BRET studies

In the BRET G-protein assay, membrane extracts taken from SH-SY5Y cells stably co-expressing the mu/RLuc and Gβ1/RGFP fusoproteins were used in concentration response experiments to evaluate receptor/G-protein interaction. Dermorphin promoted mu/G-protein interaction in a concentration dependent manner with pEC_{50} of 7.71 (7.41–8.01) and maximal effect of 0.96 ± 0.11 stimulated BRET ratio. The intrinsic activities of the compounds under study were computed as fraction of the standard ligand dermorphin maximal-stimulated BRET ratio (dermorphin = 1.00) (Fig. 2-A). All compounds, including FENT, mimicked the maximal effects of dermorphin displaying with following rank order potency: FUF ≥ FENT = OCF ≥ ACRYLF.

Whole SH-SY5Y cells stably expressing the mu/RLuc and the β-arrestin 2/RGFP fusoproteins were used to evaluate mu/β-arrestin 2 interaction. Dermorphin stimulated the interaction of the mu receptor with β-arrestin 2 in a concentration-dependent manner with pEC_{50} 6.96 (6.56–7.37) and maximal effects corresponding to 0.24 ± 0.09 stimulated BRET ratio. As for G protein studies, intrinsic activities of the

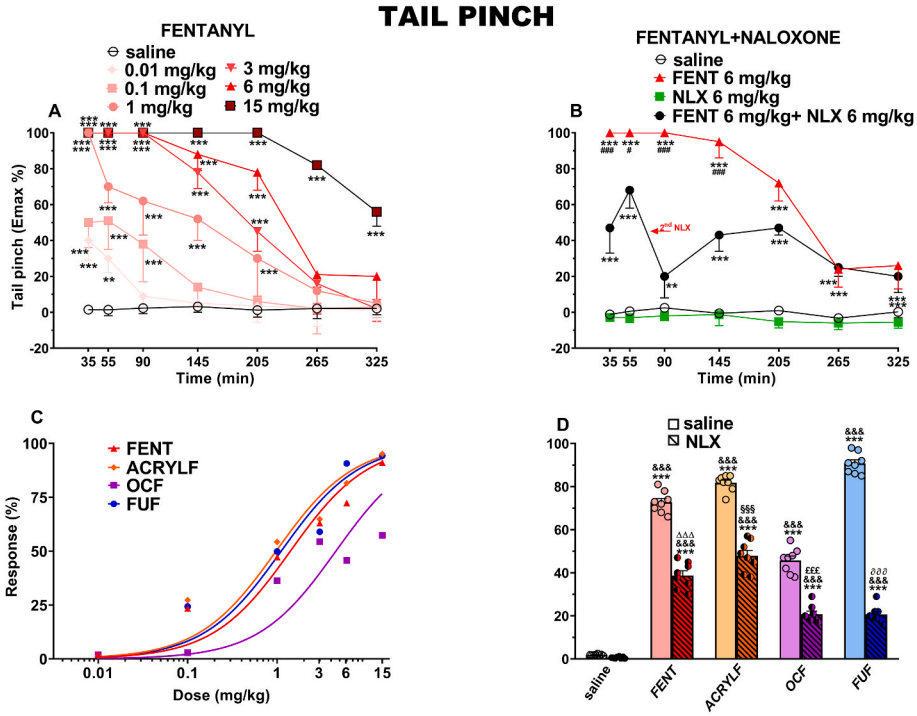

Fig. 3. Effect of the systemic administration of FENT (0.01–15 mg/kg i.p; panel A) in the tail pinch test in mice. Interaction of effective dose of FENT (6 mg/kg) with the opioid receptor antagonist NLX (panel B). Comparison of dose-response curves FENT, ACRYLF, OCF and FUF (0.01–15 mg/kg i.p; panel C). Interaction of FENT, ACRYLF, OCF and FUF (6 mg/kg) with NLX (6 mg/kg, i.p.; panel D). Data are expressed as percentage of maximum effect (see materials and methods) and represents the mean ± SEM of 8 determinations for each treatment. Statistical analysis was performed by two-way ANOVA followed by the Bonferroni's test for multiple comparisons for the dose response curve of FENT at different times (panel A and B), while the statistical analysis of panel D was performed with one-way ANOVA followed by Bonferroni test for multiple comparisons. $^{**}p < 0.01$, $^{***}p < 0.001$ versus saline; $^{\#}p < 0.05, ^{\#\#\#}p < 0.001$ versus NLX + agonist; $^{\&\&\&}p < 0.01$ versus NLX. $^{\Delta\Delta\Delta}p<0.001$ versus FENT; $^{\S\S\S}p < 0.001$ versus ACRYLF; $^{£££}p < 0.001$ versus OCF; $^{\partial\partial\partial}p < 0.001$ versus FUF.

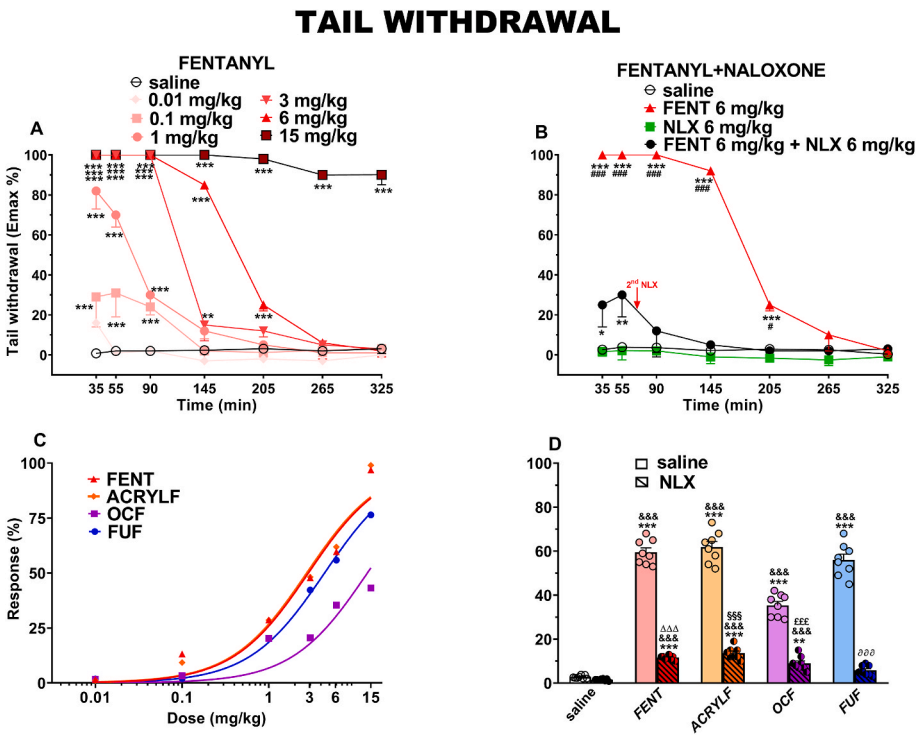

Fig. 4. Effect of the systemic administration of FENT (0.01–15 mg/kg i.p; panel A) in the tail withdrawal test in mice. Interaction of effective dose of FENT (6 mg/kg) with the opioid receptor antagonist NLX (panel B). Comparison of dose-response curves FENT, ACRYLF, OCF and FUF (0.01–15 mg/kg i.p; panel C). Interaction of FENT, ACRYLF, OCF and FUF (6 mg/kg) with NLX (6 mg/kg, i.p.; panel D). Data are expressed as percentage of maximum effect (see materials and methods) and represents the mean ± SEM of 8 determinations for each treatment. Statistical analysis was performed by two-way ANOVA followed by the Bonferroni's test for multiple comparisons for the dose response curve of FENT at different times (panel A and B) and for the comparison of the mean effects (panel C), while the statistical analysis of panel D was performed with one-way ANOVA followed by Bonferroni test for multiple comparisons. $^{**}p < 0.01$, $^{***}p < 0.001$ versus saline; $\#p < 0.05$, $\#\#\#p < 0.001$ versus NLX + agonist. $^{\&\&\&}p < 0.001$versus NLX, $^{\Delta\Delta\Delta}p<0.001$ versus FENT; $^{\S\S\S}p < 0.001$ versus ACRYLF; $^{£££}p < 0.001$ versus OCF; $^{\partial\partial\partial}p < 0.001$ versus FUF.

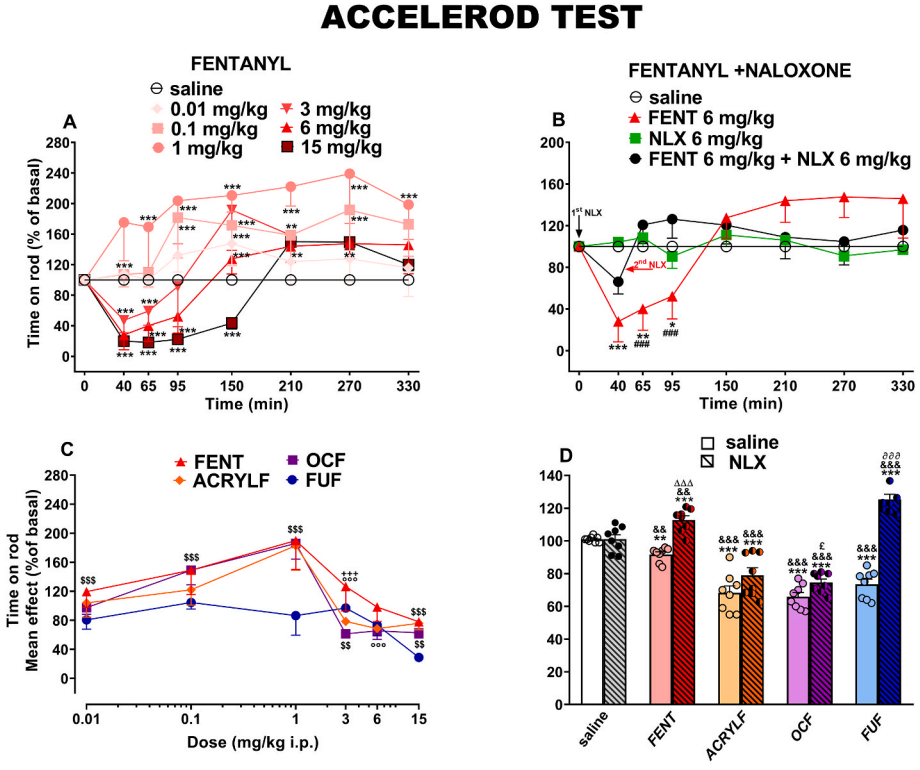

Fig. 5. Effect of the systemic administration of FENT (0.01–15 mg/kg i.p; panel A) in the Accelerod test in mice. Interaction of effective dose of FENT (6 mg/kg) with the opioid receptor antagonist NLX (panel B). Comparison of the mean effect of FENT, ACRYLF, OCF and FUF (0.01–15 mg/kg i.p) observed in 5 h (panel C). Interaction of FENT, ACRYLF, OCF and FUF (6 mg/kg) with NLX (6 mg/kg, i.p.; panel D). Data are expressed as percentage of baseline (see material and methods) and represent the mean ± SEM of 8 determinations for each treatment Statistical analysis was performed by two-way ANOVA followed by the Bonferroni's test for multiple comparisons for the dose response curve of FENT at different times (panel A and B) and for the comparison of the mean effects (panel C), while the statistical analysis of panel D was performed with one-way ANOVA followed by Bonferroni test for multiple comparisons. $^{*}p < 0.05$, $^{**}p < 0.01$, $^{***}p < 0.001$ versus saline; $\#\#\#p < 0.001$ versus NLX + agonist; $^{\circ}p < 0.001$ versus OCF. $^{\$\$}p < 0.01$, $^{\$\$\$}p < 0.001$versusFUF, $^{+++}p<0.001$versus ACRYLF; $^{\&\&}p < 0.001$, $^{\&\&\&}p < 0.001$versus NLX; $^{\Delta\Delta\Delta}p<0.001$versus FENT; $^{£}p < 0.05$ versus OCF; $^{\partial\partial\partial}p < 0.001$ versus FUF.

compounds were computed as fraction of the standard agonist dermorphin (dermorphin = 1.00) (Fig. 2-A). All compounds displayed similar potency in recruiting the β-arrestin 2 pathway (Table 2). Regarding their efficacy, all compounds behaved as partial agonists for the β-arrestin 2 pathway in comparison with dermorphin whereas FUF was completely inactive (Fig. 2-B; Table 2). Thus FUF was further investigated as an antagonist of FENT induced β-arrestin 2 recruitment. At the concentration of 0.1 μM, this compound was able to shift the concentration response curve to FENT to the right with no modification of the agonist maximal effect (See Supplementary Fig. 2); a pA_2 of 8.53 was derived from these experiments for FUF.

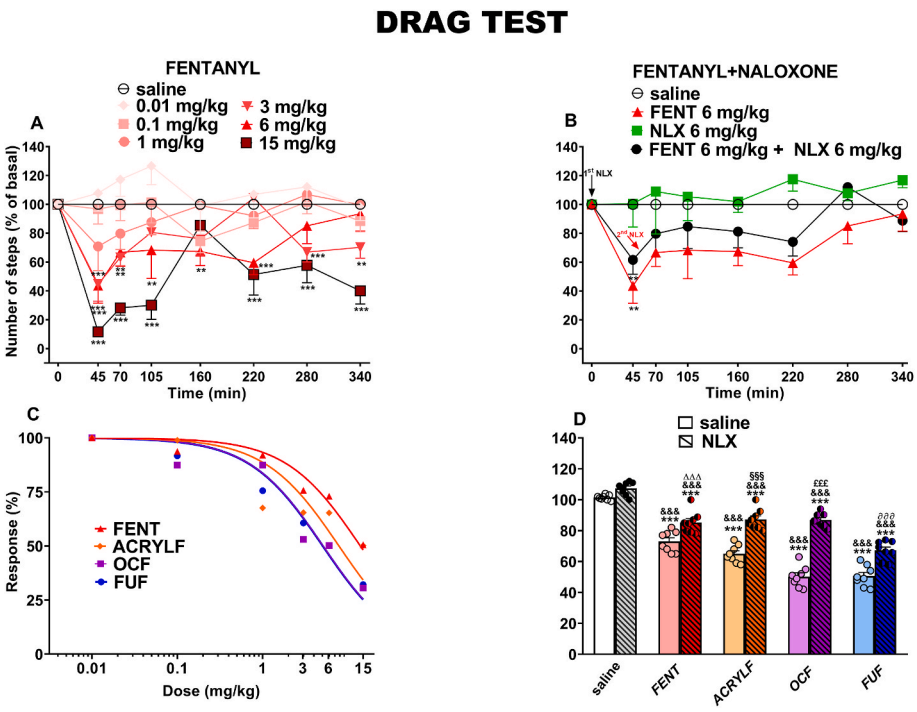

Fig. 6. Effect of the systemic administration of FENT (0.01–15 mg/kg i.p; panel A) in the Drag test in mice. Interaction of effective dose of FENT (6 mg/kg) with the opioid receptor antagonist NLX (panel B). The comparison of dose-response curves of FENT, ACRYLF, OCF and FUF (0.01–15 mg/kg i.p; panel C). Interaction of FENT, ACRYLF, OCF and FUF (6 mg/kg) with NLX (6 mg/kg, i.p.; panel D). Data are expressed as percentage of baseline (see material and methods) and represent the mean ± SEM of 8 determinations for each treatment. Statistical analysis was performed by two-way ANOVA followed by the Bonferroni's test for multiple comparisons for the dose response curve of FENT at different times (panel A and B) and for the comparison of the mean effects (panel C), while the statistical analysis of panel D was performed with one-way ANOVA followed by Bonferroni test for multiple comparisons. **p < 0.01, ***p < 0.001versus saline; &&&p < 0.001versus NLX; ΔΔΔp<0.001versus FENT; £££p < 0.001 versus OCF; ∂∂∂p < 0.001 versus FUF.

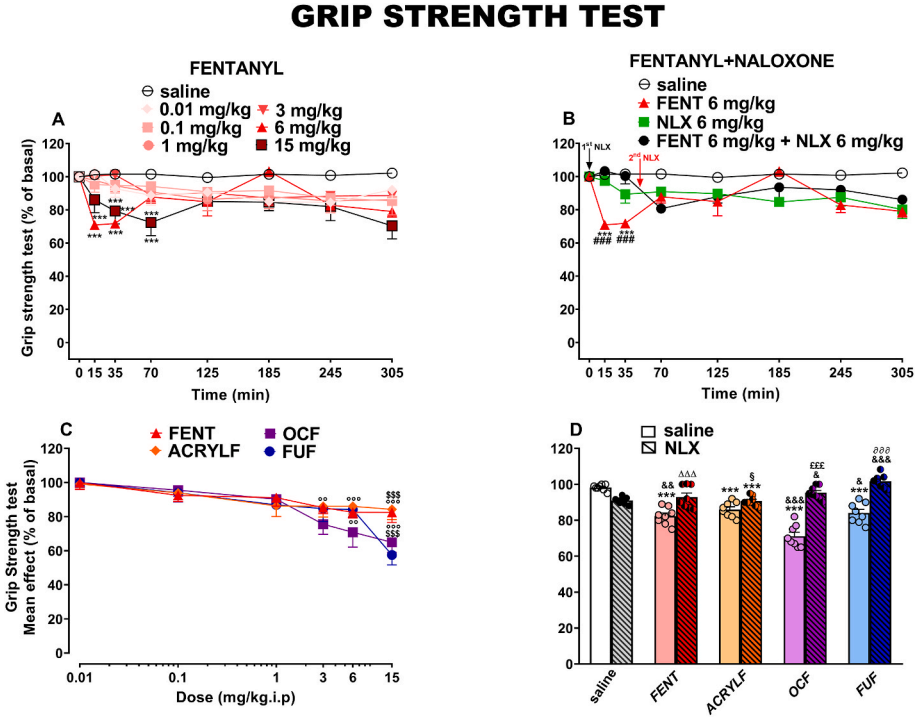

Fig. 7. Effect of the systemic administration of FENT (0.01–15 mg/kg i.p; panel A) in the Grip strength test in the mouse. Interaction of effective dose of FENT (6 mg/kg) with the opioid receptor antagonist NLX (panel B). Comparison of the mean effect of FENT, ACRYLF, OCF and FUF (0.01–15 mg/kg i.p) observed in 5 h (panel C). Interaction of FENT, ACRYLF, OCF and FUF (6 mg/kg i.p) with NLX (6 mg/kg, i.p; panel D). Data are expressed as percentage of baseline (see material and methods) and represent the mean ± SEM of 8 determinations for each treatment. Statistical analysis was performed by two-way ANOVA followed by the Bonferroni's test for multiple comparisons for the dose response curve of FENT at different times (panel A and B) and for the comparison of the mean effects (panel C), while the statistical analysis of panel D was performed with one-way ANOVA followed by Bonferroni test for multiple comparisons.***p < 0.001 versus saline; ###p < 0.001versus NLX + agonist; °p < 0.01,°p < 0.001versusOCF;$$$p < 0.001versusFUF;&p < 0.05,&&p < 0.01,&&&p < 0.001versus NLX; ΔΔΔp<0.001versus FENT; §p < 0.05versus ACRYLF,£££p < 0.001 versus OCF; ∂∂∂p < 0.001 versus FUF.

3.2. Behavioural studies

3.2.1. Evaluation of pain induced by mechanical and thermal stimuli

Acute mechanical and thermal pain stimuli were not affected in mice treated with saline (Figs. 3 and 4). Systemic administration of FENT (0.01–15 mg/kg i.p) increased the threshold to acute mechanical pain stimulus in the tail pinch test (Fig. 3-A). Mechanical analgesia was significantly affected by treatment [F6, 343 = 94.02, p < 0.0001], time [F6,343 = 42.48, p < 0.0001] and time × treatment interaction [F36,343 = 3.684, p < 0.0001]. Similar to FENT, ACRYLF, OCF and FUF increased the threshold to acute mechanical pain stimulus in a dose-dependent manner that reached the maximum at higher doses (3–15 mg/kg; see Supplementary Fig. 3)Comparison of the dose response curves to FENT in the tail pinch test (Fig. 3-C) revealed the following rank order potencies: ACRYLF ED50 0.97 mg/kg = FUF ED50 1.1 mg/kg = FENT ED50 1.4 mg/kg > OCF ED50 4.54 mg/kg.

Pre-treatment with NLX (6 mg/kg i.p; Fig 3-B) partially prevented the analgesic effect of FENT. The injection of a second dose of NLX (6

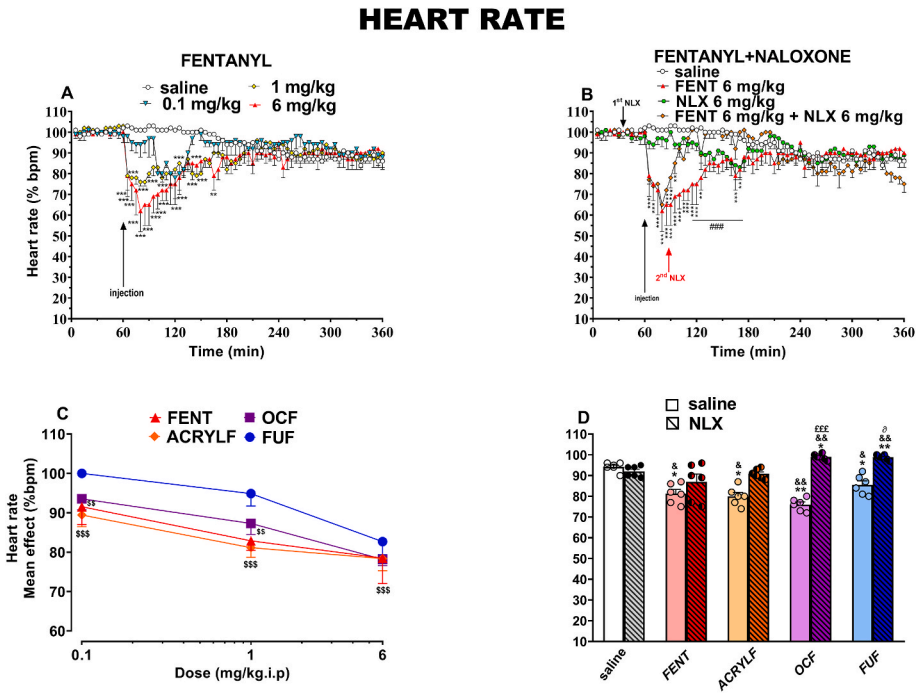

Fig. 8. Effect of the systemic administration of FENT (0.01–15 mg/kg i.p; panel A) on the heart rate in mice. Interaction of effective dose of FENT (6 mg/kg) with the opioid receptor antagonist NLX (panel B). Comparison of the mean effect of FENT, ACRYLF, OCF and FUF (0.01–15 mg/kg i.p) observed in 2 h (panel C). Interaction of FENT, ACRYLF, OCF and FUF (6 mg/kg i.p) with NLX in 5 h (6 mg/kg, i.p; panel D). Data are expressed as percentage of basal value (see material and methods) and represent the mean ± SEM of 6 determinations for each treatment. Statistical analysis was performed by two-way ANOVA followed by the Bonferroni's test for multiple comparisons for the dose response curve of FENT at different times (panel A and B) and for the comparison of the mean effects (panel C), while the statistical analysis of panel D was performed with one-way ANOVA followed by Bonferroni test for multiple comparisons. *p < 0.05,**p < 0.01 ***p < 0.001versus saline; ###p < 0.001versus NLX + agonist;$^{\$\$}$p < 0.01,$^{\$\$\$}$p < 0.001versusFUF;$^{\&}$p < 0.05,$^{\&\&}$p < 0.01versus NLX;$^{£££}$p < 0.001 versus OCF; $^{\partial}$p < 0.05 versus FUF.

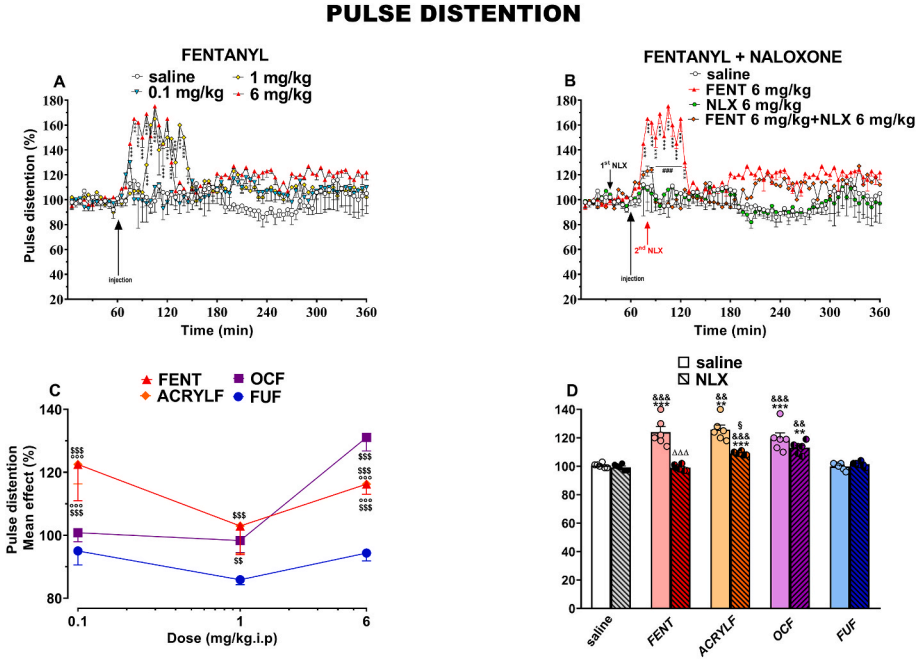

Fig. 9. Effect of the systemic administration of FENT (0.01–15 mg/kg i.p; panel A) on Pulse distention in mice. Interaction of effective dose of FENT (6 mg/kg) with the opioid receptor antagonist NLX (panel B). Comparison of the mean effect of FENT, ACRYLF, OCF and FUF (0.01–15 mg/kg i.p) observed in 2 h (panel C). Interaction of FENT, ACRYLF, OCF and FUF (6 mg/kg i.p) with NLX in 5 h (6 mg/kg, i.p; panel D). Data are expressed as percentage of basal value (see material and methods) and represent the mean ± SEM of 6 determinations for each treatment. Statistical analysis was performed by two-way ANOVA followed by the Bonferroni's test for multiple comparisons for the dose response curve of FENT at different times (panel A and B) and for the comparison of the mean effects (panel C), while the statistical analysis of panel D was performed with one-way ANOVA followed by Bonferroni test for multiple comparisons.**p < 0.01 ***p < 0.001versus saline; ###p < 0.001versus NLX + agonist; °p < 0.001versus OCF $^{\$\$}$p < 0.01,$^{\$\$\$}$p < 0.001versus FUF; $^{\&\&}$p < 0.01, $^{\&\&\&}$p < 0.001versus NLX; $^{\Delta\Delta\Delta}$p<0.001versus FENT; §p < 0.05versus ACRYLF.

mg/kg i.p; Fig 3-B) at 55 min did not totally block the analgesia induced by the agonist and the effect persisted until the end of the test [F3,196 = 214.1, p < 0.0001], time [F6,196 = 14.02, p < 0.0001] and time × treatment interaction [F18,196 = 7.054, p < 0.0001]. Similar to FENT, the second injection with NLX (6 mg/kg; Fig. 3-D) did not fully block the analgesic effect induced ACRYLF, OCF and FUF (for time-course curves see Supplementary Fig. 3).

Systemic administration of FENT (0.01–15 mg/kg i.p; Fig. 4-A) increased the threshold to acute thermal pain stimulus in the tail withdrawal test. In particular, after the administration of FENT thermal analgesia was significantly affected by treatment [F6,343 = 444.5, p < 0.0001], time [F6,343 = 153.0, p < 0.0001] and time × treatment interaction [F36, 343 = 26.34, p < 0.0001]. Similar to FENT, ACRYLF, OCF and FUF increased the threshold to acute thermal pain stimulus in a dose-dependent manner that reached the maximum at higher doses (3–15 mg/kg; see supplementary Fig. 4). Comparison of the dose-response curves to FENT in the tail withdrawal test (Fig. 4-C) revealed the following rank order potencies: ACRYLF ED50 = 2.74 mg/kg = FENT ED50 = 2.86 mg/kg > FUF ED50 = 4.39 mg/kg > OCF ED50 = 13.66 mg/kg.

Pre-treatment with NLX (6 mg/kgi.p; Fig. 4-B) partially prevented the analgesic effect of all compounds. The injection of a second dose of NLX (6 mg/kg i.p; Fig. 4-B) at 55 min did not totally block the analgesia induced by FENT [F3, 196 = 251.1, p < 0.0001], time [F6, 196 = 36.45,

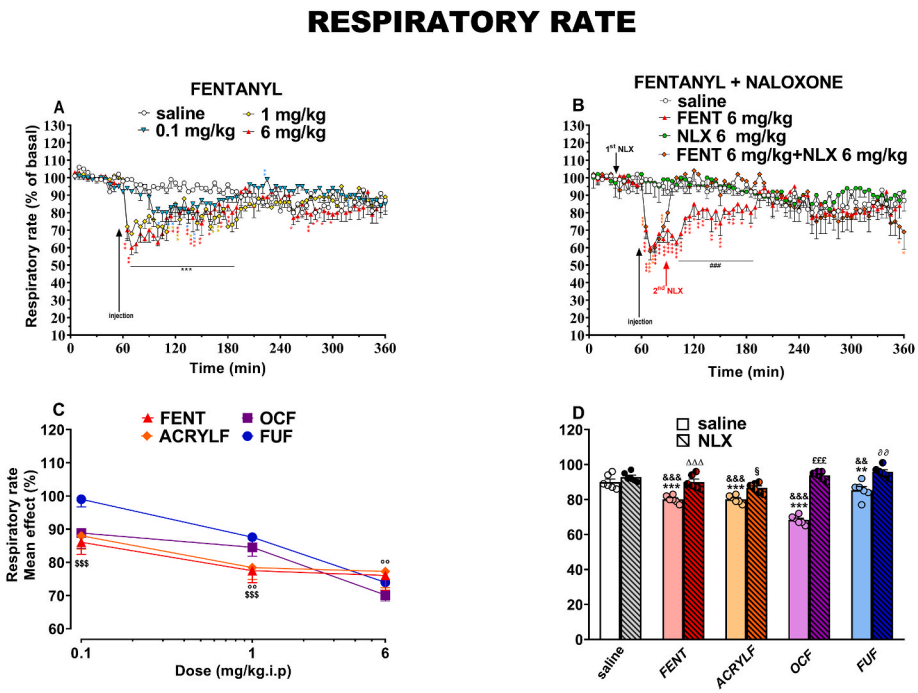

Fig. 10. Effect of the systemic administration of FENT (0.01–15 mg/kg i.p; panel A) on the Respiratory rate in mice. Interaction of effective dose of FENT (6 mg/kg) with the opioid receptor antagonist NLX (panel B). Comparison of the mean effect of FENT, ACRYLF, OCF and FUF (0.01–15 mg/kg i.p) observed in 2 h (panel C). Interaction of FENT, ACRYLF, OCF and FUF (6 mg/kg i.p) with NLX in 5 h (6 mg/kg, i.p; panel D). Data are expressed as percentage of basal value (see material and methods) and represent the mean ± SEM of 6 determinations for each treatment. Statistical analysis was performed by two-way ANOVA followed by the Bonferroni's test for multiple comparisons for the dose response curve of FENT at different times (panel A and B) and for the comparison of the mean effects (panel C), while the statistical analysis of panel D was performed with one-way ANOVA followed by Bonferroni test for multiple comparisons. *p < 0.05, **p < 0.01 ***p < 0.001versus saline; ###p < 0.001versus NLX + agonist; °p < 0.01versus OCF $^{\$\$\$}$p < 0.001versus FUF;$^{\&\&\&}$p < 0.001versus NLX; $^{\Delta\Delta\Delta}$p<0.001versus FENT; §p < 0.05versus ACRYLF;$^{£££}$p < 0.001 versus OCF; $^{\partial\partial}$p < 0.01 versus FUF.

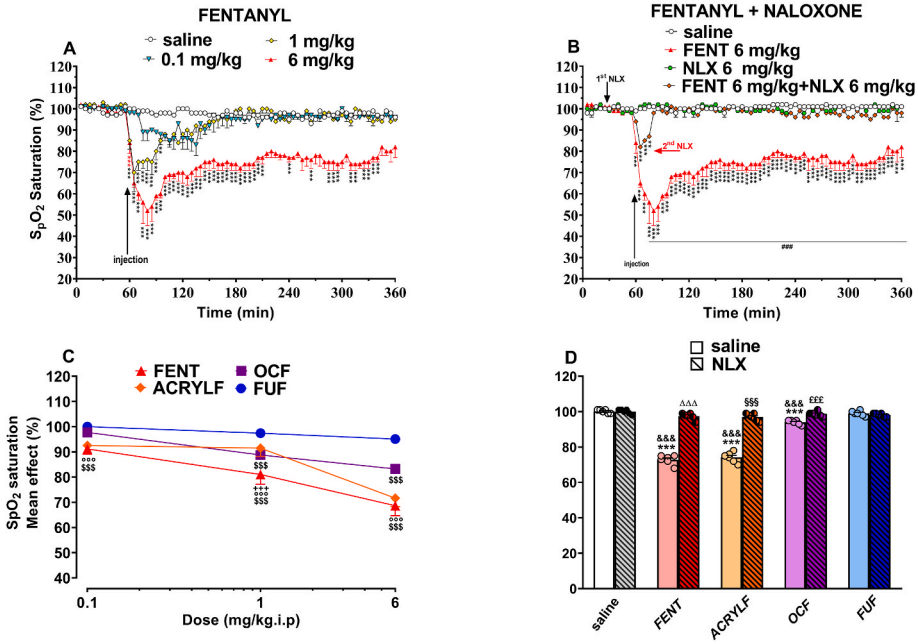

Fig. 11. Effect of the systemic administration of FENT (0.01–15 mg/kg i.p; panel A) on Oxygen saturation (SpO_2) in mice. Interaction of effective dose of FENT (6 mg/kg) with the opioid receptor antagonist NLX (panel B). Comparison of the mean effect of FENT, ACRYLF, OCF and FUF (0.01–15 mg/kg i.p) observed in 2 h (panel C). Interaction of FENT, ACRYLF, OCF and FUF (6 mg/kg i.p) with NLX in 5 h (6 mg/kg, i.p; panel D). Data are expressed as percentage of absolute value (see material and methods) and represent the mean ± SEM of 6 determinations for each treatment. Statistical analysis was performed by two-way ANOVA followed by the Bonferroni's test for multiple comparisons for the dose response curve of FENT at different times (panel A and B) and for the comparison of the mean effects (panel C), while the statistical analysis of panel D was performed with one-way ANOVA followed by Bonferroni test for multiple comparisons.**p < 0.01 ***p < 0.001versus saline; ###p < 0.001versus NLX + agonist; °p < 0.01versus OCF $^{\$\$\$}$p < 0.001versus FUF;$^{\&\&\&}$p < 0.001versus NLX; $^{\Delta\Delta\Delta}$p<0.001versus FENT; §§§p < 0.001versus ACRYLF;$^{£££}$p < 0.001 versus OCF.

p < 0.0001] and time × treatment interaction [F18, 196 = 20.99, p < 0.0001] and the effect persisted until the end of the test. As presented in Fig. 4-D, the injection of second dose of NLX (6 mg/kg) was not effective at totally blocking the analgesic effects induced by FENT, ACRYLF, OCF and FUF (for time-course curves see Supplementary Fig. 4).

3.2.2. *Evaluation of motor activity*

3.2.2.1. Accelerod test. There was no change in accelerod test performance in mice treated with saline (Fig. 5). Systemic administration of FENT (0.01–15 mg/kg i.p) significantly impaired mouse performance in the accelerod test. Similar to FENT, ACRYLF, OCF and FUF impaired performance in the accelerod test (see Supplementary Fig. 5). After administration of FENT (Fig. 5-A), the performance of mice in the accelerod was affected by the treatment [$F_{6, 343} = 12.79$], time [$F_{7, 343} = 8.031$, $P < 0.0001$] and time × treatment interaction [$F_{42, 343} = 1.146$, $P = 0.2533$]. In particular, FENT induced a biphasic effect with a facilitatory action at low doses (0.1–1 mg/kg) and an inhibitory action at higher doses (3–15 mg/kg). Comparison of the mean effect among FENT, ACRYLF, OCF and FUF (Fig. 5-C) revealed significant differences in the action of each substance at different doses [significant effect of

Table 1
Effects of dermorphin, fentanyl and its derivatives in calcium mobilization experiments performed in CHO cells coexpressing opioid receptors and the chimeric G-proteins. *p < 0.05 vs dermorphin according to ANOVA followed by the Dunnett test. Data are mean of at least 3 separate experiments made in duplicate.

	mu		Delta		kappa	
	pEC50 (CL95%)	Emax ± sem %	pEC50 (CL95%)	Emax ± sem %	pEC50 (CL95%)	Emax ± sem %
Standard agonists	8.19 (8.02–8.36)	319 ± 13	7.47 (7.09–7.85)	230 ± 18	8.81 (8.22–9.40)	257 ± 34
FENT	8.13 (7.73–8.52)	326 ± 13	CRC incomplete		CRC incomplete	
ACRYLF	8.20 (7.05–9.35)	308 ± 12	CRC incomplete		CRC incomplete	
OCF	7.78 (7.50–8.07)	305 ± 16	CRC incomplete		CRC incomplete	
FUF	7.93 (7.57–8.29)	226 ± 7*	Inactive		Inactive	

Standard agonists were dermorphin, DPDPE and dynorphin A for mu, delta and kappa opioid receptors, respectively.

Table 2
Effects of dermorphin, fentanyl and its derivatives in BRET experiments investigating mu/G protein and mu/β-arrestin 2 interaction.

	mu/G protein		mu/β-arrestin2	
	pEC_{50} ($CL_{95\%}$)	α±SEM	pEC_{50} ($CL_{95\%}$)	α±SEM
Dermorphin	7.71 (7.41–8.01)	1.00	6.96 (6.56–7.37)	1.00
FENT	8.28 (8.06–8.49)	1.11 ± 0.07	6.86 (6.54–7.18)	0.67 ± 0.02*
ACRYLF	7.87 (7.49–8.25)	1.18 ± 0.10	6.76 (6.48–7.03)	0.68 ± 0.05*
OCF	8.09 (7.63–8.55)	1.03 ± 0.07	7.28 (6.65–7.92)	
FUF	8.66 (8.15–9.16)	1.04 ± 0.09	Inactive	

treatment $F_{3,\ 166} = 48.49$, $p < 0.0001$], dose [$F_{5,\ 166} = 111.7$, $P < 0.0001$] and dose × treatment interaction [$F_{15,\ 166} = 9.547$, $P < 0.0001$]. Surprisingly, FUF induced only inhibition of motor performance at the range dose tested. Moreover, FUF resulted to be the most effective ($P < 0.001$) compared with the other compounds (for time-course curves of ACRYLF, OCF and FUF see Supplementary Fig. 5). Pre-treatment with NLX (6 mg/kg i.p; Fig. 5-B) partially reduced motor impairment induced at the dose of 6 mg/kg of FENT. Injection of a second dose of NLX (6 mg/kg i.p; Fig. 5-B) totally blocked motor impairment induced by the agonist at the dose of 6 mg/kg: FENT [$F_{3,\ 196} = 1.006$, $P = 0.3915$], time [$F_{7,\ 196} = 6.346$, $P < 0.0001$] and time × treatment interaction [$F_{21,\ 196} = 4.263$, $P < 0.0001$].The injection of a second dose of NLX at 55 min (Fig. 5-D) prevented the inhibition of motor performance in mice treated with FENT and FUF at the dose of 6 mg/kg but not in those treated with ACRYLF and OCF.

3.2.2.2. Drag test. Systemic administration of FENT (0.01–15 mg/kg i.p) reduced the number of steps performed by the front legs (Fig. 6-A). After administration of FENT, the number of steps performed was significantly affected by treatment [$F_{6,\ 343} = 31.39$, $p < 0.0001$], time [$F_{7,\ 343} = 6.703$, $P < 0.0001$] and time × treatment interaction [$F_{42,\ 343} = 2.395$, $P < 0.0001$]. Similar to FENT, ACRYLF, OCF and FUF reduced the number of the steps on the drag test (see Supplementary Fig. 6 for time-course curves). . Comparison of dose-response curves to FENT in the Drag test (Fig 6-C) revealed the following rank order of potencies: FUF ED50 = 5.07 = OCF ED50 = 5.11 mg/kg > ACRYLF ED50 = 7.82 mg/kg > FENT ED50 = 13.93 mg/kg.

The pre-treatment with NLX (6 mg/kg i.p; Fig. 6-B) partially prevented the inhibition of steps at the dose of 6 mg/kg of FENT. The injection of a second dose of NLX (6 mg/kg i.p; Fig. 6-B) at 55 min did not totally prevent the inhibitory effect induced by FENT [$F_{3,\ 196} = 14.14$, $P < 0.0001$], time [$F_{7,\ 196} = 2.319$, $P = 0.0275$] and time × treatment interaction [$F_{21,\ 196} = 0.9279$, $P = 0.5557$]. Similar to FENT, the injection of a second dose of NLX (6 mg/kg i.p; Fig. 6-D) partially prevented the inhibitory effects in mice treated with ACRYLF, OCF and FUF.

3.2.3. Evaluation of skeletal muscle strength

Muscle strength was not affected in mice treated with saline (Fig. 7). Systemic administration of FENT (0.01–15 mg/kg i.p) decreased pulling force in a dose-dependent manner (Fig. 7-A). In particular, after the administration of FENT, skeletal muscle strength was significantly affected by treatment [$F_{6,\ 343} = 20.55$, $P < 0.0001$ time [$F_{7,\ 343} = 7.630$, $P < 0.0001$] and time × treatment interaction [$F_{42,\ 343} = 2.311$, $P < 0.0001$]. Similar to FENT, ACRYLF, OCF and FUF reduced the pulling force in a dose-dependent manner (see Supplementary Fig. 7 for time-course curves). Comparison of the mean effect among FENT, ACRYLF, OCF and FUF (Fig. 7-C) revealed significant differences in the action of each substance at different doses [significant effect of treatment $F_{3,\ 166} = 13.34$, $p < 0.0001$], dose [$F_{5,\ 166} = 78.45$, $P < 0.0001$] and dose × treatment interaction [$F_{15,\ 166} = 8.292$, $P = 0.0008$]. ACRYLF was more effective than FENT and OCF at inhibiting the number of steps at the dose of 1 mg/kg. OCF was more effective than FENT and ACRYLF and FUF at the doses of 3 and 6 mg/kg and FUF was more effective than FENT and ACRYLF at the highest dose tested (15 mg/kg). Pre-treatment with NLX (6 mg/kg i.p; Fig. 7-B) partially prevented the changes in skeletal muscle force caused by FENT (6 mg/kg). The injection of a second dose of NLX (6 mg/kg i.p) totally blocked the inhibitory effect induced by FENT [$F_{3,196} = 32.86$, $P < 0.0001$), time [$F_{7,\ 176} = 5.713$, $P < 0.0001$] and time × treatment interaction [$F_{21,\ 196} = 4.578$, $P < 0.0001$]. Injection of a second dose of NLX (6 mg/kg i.p; Fig. 7-D) totally prevented the inhibitory effects in mice treated with ACRYLF, OCF and FUF.

3.2.4. Cardiorespiratory analysis

The effect of FENT on cardiorespiratory changes has been widely investigated. Using the non-invasive instrument "the MouseOX" (see Materials and Methods) we compared the effects of ACRYLF, OCF and FUF to FENT. The saline used in this experiment showed a stable profile during the 6 h of cardiorespiratory parameter measurement (heart rate, respiratory rate, oxygen saturation and pulse distention; Figs. 8–11). Systemic administration of FENT and its derivatives (0.1–6 mg/kg i.p), induced important dose-dependent variations in cardiorespiratory parameters.

Heart rate (Fig. 8) was rapidly (5 min post injection) and significantly affected by FENT (Fig. 8-A) treatment [$F_{3,\ 1584} = 70.73$, $P < 0.0001$], time [$F_{71,\ 1584} = 6.524$, $P < 0.0001$] and time × treatment interaction [$F_{213,\ 1584} = 2.985$, $P < 0.0001$]. Similar to FENT, ACRYLF, OCF and FUF reduced heart rate in a dose-dependent manner (see Supplementary Fig. 8 for time-course curves). Comparison of the mean effect among FENT, ACRYLF, OCF and FUF (Fig. 8-C), revealed significant differences in the action of each substance at different doses [significant effect of treatment $F_{3,\ 60} = 28.99$, $p < 0.0001$], dose [$F_{2,\ 60} = 109.1$, $P < 0.0001$] and dose × treatment interaction [$F_{6,\ 60} = 2.628$, $P = 0.0250$]. FUF was less effective than FENT, ACRYLF and OCF in decreasing the heart rate over the dose range tested (0.1–6 mg/kg; Fig. 8-C). Pre-treatment with NLX (6 mg/kg.i.p; Fig. 8-B) partially prevented FENT bradycardia. Injection of a second dose of NLX (6 mg/kg i.p; Fig. 8-B) totally blocked the inhibitory effect induced by FENT [significant effect of the treatment ($F_{3,\ 1440} = 76.66$, $P < 0.0001$), time ($F_{71,}$

$_{1440}$ = 8.303, P < 0.0001) and time × treatment interaction ($F_{213,\ 1440}$ = 4.103, P < 0.0001]. Similar to FENT, injection of second dose of NLX (6 mg/kg i.p; Fig. 8-D) totally prevented bradycardia induced by ACRYLF, OCF and FUF.

Pulse distention (Fig. 9) in the group of mice treated with FENT (Fig. 9-A) was significantly affected by treatment [$F_{3,\ 1584}$ = 91,14, P < 0,0001], time [$F_{71,\ 1584}$ = 4.870, P < 0.0001] and time × treatment interaction [$F_{213,\ 1584}$ = 2.427, P < 0.0001]. Comparison of mean effect among FENT, ACRYLF, OCF and FUF (Fig. 9-C), revealed significant differences in the action of each substance at different doses [significant effect of treatment $F_{3,\ 60}$ = 57.41, p < 0.0001], dose [$F_{2,\ 60}$ = 53.41, P < 0.0001] and dose × treatment interaction [$F_{6,\ 60}$ = 14.06, P < 0.0001]. FUF did not affect pulse distention. FENT and ACRYLF are more effective than OCF at the dose of 0.1 mg/kg, while OCF was more effective than FENT and ACRYLF at the dose of 6 mg/kg.

Pre-treatment with NLX (6 mg/kg i.p; Fig. 9-B) partially prevented the increase in pulse distention caused by FENT, ACRYLF and OCF. Injection of a second dose of NLX (6 mg/kg i.p; Fig. 9-B) totally blocked the changes in pulse distention induced by: FENT [$F_{3,\ 1440}$ = 130,0, P < 0,0001], time [$F_{71,\ 1440}$ = 3,193, P < 0,0001] and time × treatment interaction [$F_{213,\ 1440}$ = 2,239, P < 0,0001]. Similar to FENT, the injection of second dose of NLX (6 mg/kg i.p; Fig. 9-D) totally prevented the increase in Pulse distention induced by ACRYLF and OCF.

After the administration of FENT, respiratory rate (Fig. 10-A) was also significantly affected by treatment: [$F_{3,\ 1584}$ = 91.01, P < 0.0001], time [$F_{71,\ 1584}$ = 12.86, P < 0.0001] and time × treatment interaction [$F_{213,\ 1584}$ = 3.614, P < 0.0001]. Comparison of the mean effect among FENT, ACRYLF, OCF and FUF (Fig. 10-C) revealed significant differences in the action of each substance at different doses [significant effect of treatment $F_{3,\ 60}$ = 13.89, p < 0.0001], dose [$F_{2,\ 60}$ = 124.1, P < 0.0001] and dose × treatment interaction [$F_{6,\ 60}$ = 9.041, P < 0.0001]. FUF was less effective than FENT, ACRYLF at the dose of 0.1 and 1 mg/kg. OCF was less effective than FENT, ACRYLF at the dose of 1 mg/kg, while OCF was more effective than ACRYLF at the dose of 6 mg/kg. Pre-treatment with NLX (6 mg/kg i.p; Fig. 10-B) partially prevented the bradypnea caused by FENT. Injection of a second dose of NLX (6 mg/kg i.p; Fig. 10-B) totally blocked the inhibitory effect induced by FENT [$F_{3,\ 1440}$ = 57.67, P < 0.0001], time [$F_{71,\ 1440}$ = 6.925, P < 0.0001] and time × treatment interaction [$F_{213,\ 1440}$ = 2.241, P < 0.0001]. Similar to FENT, the injection of a second dose of NLX (6 mg/kg.i.p; Fig. 10-D) totally prevented bradpnea induced by ACRYLF, OCF and FUF.

After administration of FENT (Fig. 11-A), oxygen saturation was significantly affected by treatment [$F_{3,\ 1584}$ = 1246, P < 0,0001], time [$F_{71,\ 1584}$ = 22.63, P < 0.0001] and time × treatment interaction [$F_{213,\ 1584}$ = 6.819, P < 0.0001]. Comparison of the mean effect among FENT, ACRYLF, OCF and FUF (Fig. 11-C) revealed significant differences in the action of each substance at different doses [significant effect of treatment F3, 60 = 176.9, p < 0.0001], dose [F 2, 60 = 277.9, P < 0.0001] and dose × treatment interaction [F6, 60 = 26.51, P < 0.0001]. In contrast to FENT, ACRLF and OCF, FUF did not affect the oxygen saturation over the dose range 0.1–6 mg/kg. FENT and ACRLF were more effective than OCF at the doses of 0.1 and 6 mg/kg while FENT was more effective than ACRYLF and OCF at the dose of 1 mg/kg.

Pre-treatment with NLX (6 mg/kg i.p; Fig. 11-B) partially prevented by FENT (6 mg/kg) SpO_2 changes. Injection of a second dose of NLX (6 mg/kg i.p; Fig. 11-B) totally blocked the inhibitory effects induced by FENT [treatment [$F_{3,\ 1440}$ = 2508, P < 0.0001], time [$F_{71,\ 1440}$ = 11.58, P < 0,0001] and time × treatment interaction [$F_{213,\ 1440}$ = 9.521, P < 0.0001]. Similar to FENT, injection of a second dose of NLX (6 mg/kg i.p; Fig. 11-D) totally prevented the inhibitory effects induced by ACRYLF, OCF and FUF.

4. Discussion

Our study presents novel results regarding the in vitro and in vivo characterization of ACRYLF, OCF and FUF, three FENT analogues that have recently emerged as NPS. In vitro, in the calcium mobilization assay the three FENS were able to activate the mu opioid receptor in a concentration dependent manner and all compounds were able to elicit maximal effects similar to that of dermorphin, with the exception of FUF that behaved as a partial agonist. In the BRET G-protein assay, all compounds, including FENT, mimicked the maximal effects of dermorphin. FENT, ACRYLF and OCF behaved as partial agonists for the β-arrestin 2 pathway in comparison to dermorphin whereas FUF was inactive in promoting β-arrestin 2 recruitment. In vivo, all compounds increased mechanical and thermal analgesia, altered motor performance (facilitation at low and inhibition at higher doses) and impaired cardiorespiratory parameters in mice. Of note, FUF showed lower potency for inhibiting cardiorespiratory function and exerted only a monophasic inhibitory action on motor activity. NLX sensitivity of the actions of FENT and its derivatives was variable depending on both the biological function examined and substance used.

4.1. Analgesic effects

The efficacy of FENT as a potent analgesic has been extensively documented in preclinical and clinical studies. The new FENS have also been investigated for their analgesic properties. Our study demonstrates that FENT and its derivatives induce a dose-dependent increase in the threshold to acute mechanical and thermal pain stimulus. Comparison of the dose response curves in the tail pinch (Fig. 3) and withdrawal (Fig. 4) tests demonstrated no major differences in term of analgesic potency between FENT, ACRYLF and FUF. OCF showed the highest ED_{50} value and shorter duration of action. This is in line with previous findings since OCF has been reported to have a shorter duration of action in the mouse hot-plate test compared to FENT (Bagley et al., 1991). However, contrary to our findings; Bagley et al. showed a higher potency of OCF in comparison to FENT in this test. The difference in potency could be related to differences in experimental protocols and the species used (Baumann et al., 2018). Moreover, our data demonstrated analgesic efficacy of FUF corroborating previous findings that suggested high analgesic potency after i.v. administration in the mouse hot plate test (Huang et al., 1986). Pre-treatment for 15 min with 6 mg/kg NLX did not prevent the antinociceptive effect of 6 mg/kg of FENT, ACRYLF, OCF and FUF (Fig. 3-B and D). In the tail pinch test, the pre-treatment seemed to significantly reduce the analgesic effect of FUF but not the other compounds. Neither the second injection of 6 mg/kg of NLX at 55 min of treatment blocked the threshold to mechanical analgesia in mice (Fig. 3-D). The antagonist profile of NLX is somewhat different in the tail withdrawal test (Fig. 4). In fact, the pre-treatment with 6 mg/kg with NLX fully prevented the thermal analgesia induced by FUF and significantly reduced the analgesic effect with the other compounds, the second dose of NLX totally blocked thermal analgesia induced by FENT, ACRYLF and OCF (Fig. 4-B and D). These results confirm the involvement of mu opioid receptors in the analgesia induced by FENT and its analogues. Indeed, a recent study using genetically-engineered mice lacking specific splice variants of MOR-1(E1/E11 KO mice) revealed that butyrylfentanyl and other opioids failed to promote analgesic effects in the radiant heat tail flick test when compared to the wild type mice (Baumann et al., 2018).

A difference in pharmacokinetics of these molecules has been noticed in both tests, where OCF showed a short analgesic action in respect to other molecules and these differences could be related to their chemical structures (Wilde et al., 2019; Varshneya et al., 2022). Moreover, the higher efficacy of NLX in blocking the analgesic effects of the FENT, ACRYLF and OCF in the tail withdrawal test compared to the tail pinch test could be related to differences in the intensity of the nociceptive stimuli that results in differences in NLX efficacy for blocking pain sensitivity in the two tests (Le Bars et al., 2001). The mechanisms by which opioids induce analgesia have been widely studied in animal models (Lazorthes et al., 1988; Besson et al., 1992; Stein et al., 2003; Aoki et al., 2014) and have confirmed that mu agonists produce

analgesia through both pre- and postsynaptic mechanisms at multiple CNS sites (Torrecilla et al., 2002). Moreover, it has been well documented that opioids can directly block pain transmission at the spinal cord level, acting on primary afferents (Wall, 1967; Zollner et al., 2003; Sun et al., 2020) and nociceptive relay neurons in the dorsal horn (Glaum et al., 1994).

4.2. Motor effects

Systemic administration of FENT, ACRYLF, OCF and FUF dose-dependently affects the motor performance in mice (Fig. 5). The data obtained in the accelerod test show a biphasic effect of all FENS but not for FUF (Supplementary Fig. 5). However, in the drag test (Fig. 6-C), the effect of all compounds was only inhibitory with the following rank of ED_{50}: FUF ($ED_{50} = 5.07$ mg/kg) = OCF ($ED_{50} = 5.11$ mg/kg) > ACRYLF ($ED_{50} = 7.82$ mg/kg) ≥ FENT ($ED_{50} = 13.93$ mg/kg). As reported in our previous study opioid agonists elicited variable effects in the accelerod and drag test (Bilel et al., 2020). Hence, the data obtained in the accelerod test are in accordance with a recent study by Varshneya and colleagues. It has been reported in the spontaneous locomotion test that FENT at the dose of 1 mg/kg induces hyperlocomotion which is inverted at higher doses (Varshneya et al., 2019). In rodents, opioids can induce a biphasic effect depending on the dose, the time after injection and the test used (Essawi, 1998; Rodriguez-Arias et al., 2000; Bilel et al., 2020; Pesavento et al., 2022). The interaction of the opioidergic system with other systems like the dopaminergic and serotonergic systems are still under investigation. Yet, one of the mechanisms related to the facilitation of locomotion by opioid agonists is triggered by the activation of the mesolimbic dopaminergic system which is regulated by the endogenous opioid system, controlling the release of dopamine in the nucleus accumbens (Di Chiara & Imperato, 1988; Matsui et al., 2014). Indeed, a recent elegant study revealed that the highly potent FENT interacts with dopamine (D_1 and D_4) receptors in the low micromolar range (Torralva et al., 2020). Moreover, FENT activates serotonin receptors (5-HT1A) at low concentrations (Martin et al., 1991; Torralva et al., 2020). Yet, FENT, ACRYLF and OCF could increase locomotion involving the opioid-serotonin system (Gurtu et al., 1990). The pre-treatment with NLX did not block the inhibitory effects induced by all FENS on the motor performance of mice. The injection of the second dose at 55 min prevented the inhibitory effects induced by FENT and FUF but not that induced by ACRYLF and OCF (Fig. 5-D). These data suggest that the chemical substituent of FENT analogues could play an important role on their opioid receptor occupancy in response to various tests (Wilde et al., 2019; Varshneya et al., 2019, 2022).

The results obtained in the drag test (Fig. 6) revealed a dose-dependent reduction in the number of steps of all compounds. The drag test evaluates the ability of the mouse to balance its body posture using its forelimbs in response to a dynamic stimulation imposed by "tail dragging". Pre-treatment with NLX did not block the inhibitory effects induced by all FENS in the drag test. The injection of the second dose at 55 min did not prevent the inhibitory effects induced by all compounds (Fig. 6-D). In addition to the pharmacokinetic differences of these molecules, the results obtained with NLX antagonism in the drag test suggest a non-opioid mechanism that could be activated by these FENS in the test of motor coordination (Hustveit, 1994; Kitamura et al., 2016; Torralva et al., 2020).

We also hypothesized that the number of steps were reduced due to the muscle rigidity as previously reported with other opioids (Bilel et al., 2020). Muscle rigidity has been majorly reported in cases with respiratory depression after FENT use (Torralva and Janowsky, 2019). Indeed, FENS may produce a rigidity in the diaphragm, chest wall, and upper airway, known as wooden chest syndrome (WCS) (Çoruh et al., 2013; Torralva and Janowsky, 2019). Unexpectedly, the grip strength test (Fig. 7) revealed an inhibition of the muscle strength after the injection of all the compounds in a dose-dependent manner and the effect persisted with higher doses (6 and 15 mg/kg) for the whole observation period. The analysis of our results by all the operators shows that the animals were not able to grip the grid and this could be related to hypo-tonicity of the muscles (Chaillet et al., 1983; Weinger et al., 1988; Lui et al., 1989). Indeed, as discussed below, the three opioids induced very important impairment of cardiovascular parameters that could potentially elicit a decrease of muscle strength. On this basis we speculate that the grip strength test is not predictive for muscle rigidity in case of FENS and could lead to false interpretations. Pre-treatment with NLX totally prevented inhibitory effects in the grip strength test and this data reveals that mu opioid receptors are responsible of the hypotonic tone in mice. Opioids and in particular FENS could induce hypotonic immobility in mice through the mu receptors located in the nucleus raphe pontis and the caudate nucleus (Blasco et al., 1986). Moreover, it has been demonstrated that supraspinal delta-1 and kappa-1 play an important role in inducing muscle rigidity after FENT administration (Vankova et al., 1996). Fentanyl's interacts with cholinergic system by blocking the acetylcholine release. This mechanism could be blocked by mu antagonists like NLX (Sakai et al., 2002). Indeed, the cholinergic system could also be involved in the alterations of the muscles activity of mice after FENS injections (Sakai et al., 2002; Sohn et al., 2004).

4.3. Cardio-respiratory effects

Cardiorespiratory alterations in preclinical studies following the administration of opioids, particularly FENT's have been well established (Yadav et al., 2018; Hill et al., 2020). We have demonstrated using the MouseOX instrument that FENT, ACRYLF, OCF and FUF significantly and dose-dependently altered the cardiorespiratory parameters (Figs. 8–11) when administered to mice in the range doses 0.1–6 mg/kg. FUF did not alter pulse distention (data not shown). Pre-treatment with a single dose of NLX did not fully prevent bradycardia (Fig. 8-D) and vasodilatation (PD; Fig. 9-D) induced by these opioids, while the second dose of NLX reversed these alterations. Our data demonstrate the role of mu receptors in cardiovascular function (Varshneya et al., 2022). Many clinical studies have reported cardiovascular symptoms after FENT injection, including bradycardia and hypotension, QTc interval prolongation myocardial ischemia (Doshi et al., 2019; Helander et al., 2017). A recent study in USA revealed that of 430 patients hospitalized with opioid overdose found an association with ischemic events, heart failure, and arrhythmias (reviewed in Frisoni et al., 2018; Krantz et al., 2021). The mechanism by which opioids induce bradycardia have been reported in our previous study (Bilel et al., 2020). Moreover, all the opioids reduced respiratory rate and Oxygen saturation (Figs. 10 and 11). FUF showed lower efficacy in respect to the other molecules in the BR (Fig. 10-C) and no effect on the SpO2 saturation. In accordance with our data, Varshneya et al. demonstrated that 3-FUF induced hypoventilation with an efficacy ($ED_{50} = 2.6$ mg/kg) lower than Fentanyl ($ED_{50=}0.96$; Varshneya et al., 2022). These data reveal the role of the furan structure in changing the activity of FENT (Eshleman et al., 2020). A second dose of NLX was also needed to reverse respiratory depression by FENS confirming preclinical studies (Yadav et al., 2018; Hill et al., 2020) and clinical reports from studies showing that high NLX doses may be required to reverse FENT overdose (Rzasa Lynn and Galinkin, 2018; Somerville et al., 2017). One of the mechanical mechanisms by which opioids induce respiratory depression is the chest wall rigidity (Çoruh et al., 2013). The mechanism has shown that it is mediated by activation of mu receptors (Vankova et al., 1996; Soares et al., 2014; Varshneya et al., 2022).

FUF seemed to be the FENT derivative with lower cardiovascular toxicity in respect to ACRYLF and OCF. Various mechanisms have been suggested to understand how FENT alters cardio-respiratory function. A recent study revealed a role of β–arrestin 2 in heterologous desensitization of cardiac-β-adrenergic receptors (βAR) that could impair cardiac function and demonstrated that the ablation of β-arrestin 2 gene rescues β -adrenergic stimuli-induced myocyte contractile function (Shi et al., 2017). Moreover, it is well established that hypoxemia induced

vasodilatation in humans is attributed by β adrenergic receptors (Blauw et al., 1995). Thus the alterations of pulse distention and Oxygen saturation induced by FENT, ACRYLF and OCF but not FUF could be attributed to a crosstalk between β adrenergic receptors and mu opioid receptors via β arrestin 2 signaling in the cardiovascular system (Shi et al., 2017; Gill et al., 2019; Torralva et al., 2020).

4.4. Comparison of the profile of action of FENS

Our in vivo experiments revealed differences in the pharmacotoxicological profile of the compounds tested (Fig. 12). In particular, ACRYLF behaved more similarly to FENT than the other compounds. It has been suggested that the acrylamide moiety of ACRYLF could lead to irreversible receptor binding and higher toxicity (Essawi, 1999). However, our in vitro results demonstrate full agonism for ACRYLF with a similar potency to FENT at mu receptors. Moreover, in vivo, ACRYLF induced the same effects to FENT in analgesia, motor and cardiorespiratory changes. These results suggest that the addition of acrylamide moiety to FENT may not induce significant changes in the FENT pharmacodynamics (Watanabe et al., 2017). In contrast, OCF showed a lower potency in vitro while in vivo the effects of OCF were different in the physiological and behavioural tests. Interestingly the analgesic effect of OCF was relatively short lasting while its actions on motor and cardiorespiratory functions were persistent. The differences in toxic effects of OCF compared to FENT in animals and humans are still under debate. Preclinical studies suggested lower toxicity of OCF (Huang et al., 1986; Bagley et al., 1991) while clinical studies did not (Fletcher et al., 1991). Ocfentanyl has two modifications compared to FENT: replacement of the propionamide group with a methoxyacetamide and the addition of ortho-fluorine to the N-phenyl ring. Our data suggest that these modifications could be responsible for the changes in the pharmacodynamics of OCF especially in cardiorespiratory function which suggests high respiratory and cardiac toxicities that could induce major fatalities (Coopman et al., 2016; EMCDDA, 2017).

Furanylfentanyl is the compound displaying the most divergent pharmacological profile compared to FENT and the other analogues. In fact, in vivo FUF was the only compound with no motor stimulatory effects and the only compound that did not alter pulse distention and oxygen saturation in cardiorespiratory measurements. Moreover, FUF displayed a distinct pharmacological profile also in vitro acting as partial agonist in calcium mobilization studies and as a mu agonist strongly biased toward G protein in BRET studies. This profile for FUF is worthy of further discussion. Classical studies of the Bohn research group performed using β-arrestin 2 gene knockout mice (βarr2(−/−)) suggested that the analgesic properties of mu agonists depend on G protein signaling while side effects such as respiratory depression and constipation on βarr2 signaling (Bohn et al., 1999; Raehal et al., 2005). The logical consequence of this hypothesis is that mu receptor agonists biased toward G protein may act as safer opioid analgesics. This has been corroborated through the identification of novel mu ligands including oliceridine (TRV130) (DeWire et al., 2013), PZM21 (Manglik et al., 2016) and SR–17018 (Schmid et al., 2017) that behaved in vitro as G protein biased agonists and displayed in vivo a larger therapeutic index compared to classical opioid drugs such as morphine or FENT. Importantly oliceridine has recently been approved by the FDA for intravenous use in moderate to severe pain in adults (Lambert and Calò, 2020). However, recent data questioned the above mentioned hypothesis. In fact, the higher therapeutic index of morphine in βarr2(−/−) mice has not been confirmed by a consortium of three laboratories (Kliewer et al., 2020). Moreover, a very elegant study demonstrated that mice genetically engineered with G-protein-biased mu receptors display increased sensitivity to both the analgesic actions and side effects of opioid drugs (Kliewer et al., 2019). In addition, a very rigorous pharmacological study comparing the in vitro and in vivo actions of opioid drugs including oliceridine, PZM21, and SR–17018 demonstrated a robust correlation between their therapeutic indices and their efficacies, but not their bias factors (Gillis et al., 2020a). Therefore, the importance of biased vs partial agonism in the search for safer opioid analgesics is still an open question (Azevedo Neto et al., 2020, 2021; Gillis et al., 2020b; Vandeputte et al., 2020). We propose that FUF should be added to the panel of mu receptor ligands useful for performing further studies in this very important field of research.

Tolerance is an important factor that is highly implicated on opioid abuse. Indeed, it is well documented that FENT induces tolerance and physical dependence in a rapid and robust manner compared to morphine and other opioids (Bohn et al., 2004; Raehal and Bohn, 2011). Moreover, it has been reported in a recent elegant study the role of β-arrestin 2 in the severity of antinociceptive tolerance and physical dependence (Raehal and Bohn, 2011). Yet, FENT analogues in particular ACRYLF and OCF can induce tolerance and dependence in abusers like

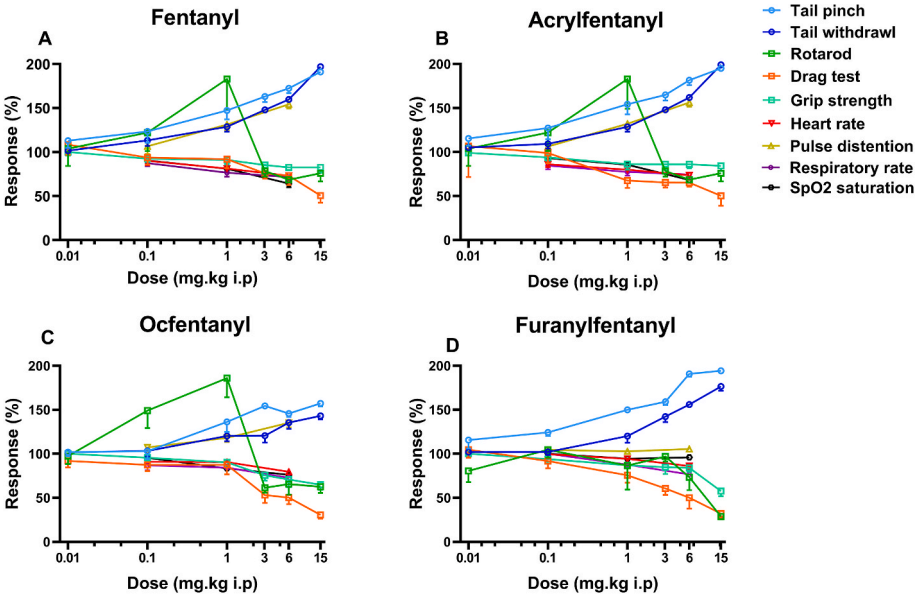

Fig. 12. Dose response curves to FENT (panel A), ACRYLF (panel B), OCF (panel C) and FUF (panel D) on the tail pinch test, tail withdrawal test, accelerod, drag test, grip strength and cardiorespiratory parameters (heart rate, pulse distention, respiratory rate and oxygen saturation) in mice.

FENT via intracellular mechanisms that involves β-arrestins signaling (Bohn et al., 2004; Raehal& Bohn, 2011) and thus increasing their risk of abuse toxicity and death with overdose (Helander et al., 2017; Kuczyńska et al., 2018; Frisoni et al., 2018). Future studies on tolerance of FENS are needed to better understand their abuse liability.

4.5. Naloxone antagonism

The present findings demonstrate that the analgesic, motor and cardiorespiratory actions of FENT as well as of FENS are sensitive to NLX; this suggest the involvement of opioid receptors, particularly the mu receptor, in these actions. However, NLX efficacy in blocking the effects of FENS was variable in the different assays. At this regard is should be underlined that NLX behaves as a competitive opioid receptor antagonist therefore its final effect depends on the relative antagonist/agonist ratio of concentrations in the brain areas controlling the different functions (Nakamura et al., 2020; Walker et al., 2021). Indeed, many factors are involved in FENT 's affinity for and the kinetics of its association and dissociation with the opioid receptor which greatly impact its reversal by naloxone (Yassen et al., 2007; Varshneya et al., 2022). Naloxone transfers and equilibrates rapidly between the plasma and the brain, and has a blood effect-site equilibration half-life of 5 min comparable to that of FENT. Yet, in rats, the brain mu receptors occupancy by intravenous (IV) NLX was greater than 90% at 5 min for clinically relevant doses of IV administered NLX (0.035 mg/kg, Human Equivalent Dose (HED) 0.4 mg; 0.17 mg/kg, HED 2 mg). Only 50% occupancy remained at 27.3 min and at 85 min after 0.035 mg/kg and 0.17 mg/kg NLX, respectively (Research report by Kang et al., 2022). In humans a dose of 1 mg in an 80 kg individual of NLX will occupy 50% of available receptor sites in the human brain and since NLX is a competitive antagonist at the mu-opioid receptor, this dose may be insufficient to reverse toxicity (respiratory depression) due to very large doses of FENS and their higher affinity for the mu-opioid receptor, in which very few opioid binding sites remain unoccupied (Yassen et al., 2007). Moreover, it is suggested in clinical cases of FENT overdose to use a repeat NLX dosing in order to avoid the reappearance of the effects (Klebacher et al., 2017). Thus the above mentioned evidences may likely explain the different effects of NLX in blocking FENS actions in comparison with other opioids e.g. morphine (Bilel et al., 2020). On the other hand, our findings do not rule out that non-opioid mechanisms might be involved into the in vivo actions of FENS as suggested by recent studies (Baumann et al., 2018; Varshneya et al., 2022). This issue can be eventually addressed in future studies by comparing the in vivo actions of FENT and FENS in wild type and in mice knockout for the mu receptor gene.

5. Conclusions

The present study demonstrates that ACRYLF, OCF and FUF, behave similarly to FENT as mu opioid agonists. In contrast to FENT and the other analogues, FUF acts as a partial agonist in vitro at mu opioid receptors, and as G protein biased mu agonist; this is associated with lower potency in vivo in cardiorespiratory depression. Collectively our data reveal the high risk associated with the use of these compounds and the strong relationship between the chemical structure and the pharmacotoxicology of fentanyl analogues, a drug class playing an important role in the current opioid epidemic.

Funding sources

This research was supported by the Anti-Drug Policies Department, Presidency of the Council of Ministers, Italy (project: "Effects of NPS: development of a multicentre research for the information enhancement of the Early Warning System" to M. Marti), by local funds from the University of Ferrara (FAR, 2019 and FAR, 2020 to M. Marti; FAR, 2020 to G Calo'), by FIRB 2012 from the Italian Ministry of Education, University and Research (Grant no. RBFR12LDOW to F. De-Giorgio) and by local funds from the Catholic University of Rome (Linea D1 grants to F. De-Giorgio).

Credit author statement

Matteo Marti, Sabrine Bilel, Girolamo Calò contributed conception and design of the study. Sabrine Bilel, Micaela Tirri, Raffaella Arfè, Tatiana Bernardi, Federica Boccuto, Beatrice Marchetti, Giorgia Corli performed in vivo experimental section. Joaquim Azevedo Neto, Davide Malfacini performed in vitro experimental section. Matteo Marti, Sabrine Bilel, Girolamo Calò wrote the manuscript. Giovanni Serpelloni, Fabio De-Giorgio, Rosa Maria Gaudio, edited sections of the manuscript. Sabrine Bilel, Matteo Marti, Micaela Tirri, Raffaella Arfè, Tatiana Bernardi, Federica Boccuto performed statistical analysis. Matteo Marti, Sabrine Bilel, Girolamo Calò and Davide Malfacini contributed to manuscript revision, read and approved the submitted version.

Ethical statements

All applicable international, national and/or institutional guidelines for the care and use of animals were followed. All procedures performed in the studies involving animals were in accordance with the ethical standards of the institution or practice at which the studies were conducted. Project activated in collaboration with the Presidency of the Council of Ministers-DPA Anti-Drug Policies (Italy).

Declaration of competing interest

The Authors declare no conflict of interest.

Acknowledgements

We would like to thank Professor David Lambert (Department of Cardiovascular Sciences, Anesthesia, Critical Care and Pain Management, University of Leicester, Leicester LE1 7RH, UK) for the revision of our manuscript.

Appendix A. Supplementary data

Supplementary data to this article can be found online at https://doi.org/10.1016/j.neuropharm.2022.109020.

References

EMCDDA, 2016. European Drug Report 2016: Trends and Developments. Publications Office of the European Union, Luxembourg.

EMCDDA, 2017. European Drug Report 2017: Trends and Developments. Publications Office of the European Union, Luxembourg.

EMCDDA, 2019. European Drug Report 2019: Trends and Developments. Publications Office of the European Union, Luxembourg.

Aoki, Y., Mizoguchi, H., Watanabe, C., Takeda, K., Sakurada, T., Sakurada, S., 2014. Potential involvement of mu-opioid receptor dysregulation on the reduced antinociception of morphine in the inflammatory pain state in mice. J. Pharmacol. Sci. 124 (2), 258–266. https://doi.org/10.1254/jphs.13242fp.

Azevedo Neto, J., Costanzini, A., De Giorgio, R., Lambert, D.G., Ruzza, C., Calò, G., 2020 Aug 25. Biased versus partial agonism in the search for safer opioid analgesics. Molecules 25 (17), 3870. https://doi.org/10.3390/molecules25173870.PMID:32854452;PMCID:PMC7504468.

Azevedo Neto, J., Ruzza, C., Sturaro, C., Malfacini, D., Pacifico, S., Zaveri Nurulain, T., Calò, G., 2021 March. Functional selectivity does not predict antinociceptive/locomotor impairing potencies of NOP receptor agonists. Front. Neurosci. https://doi.org/10.3389/fnins.2021.657153.

Bagley, J.R., Kudzma, L.V., Lalinde, N.L., Colapret, J.A., Huang, B.-S., Lin, B.-S., Jerussi, T.P., Benvenga, M.J., Doorley, B.M., Ossipov, M.H., Spaulding, T.C., Spencer, H.K., 1991. Evolution of the 4-anilidopiperadine class of opioid analgesics. Med. Res. Rev. 11 (4), 403–436.

Baumann, M.H., Majumdar, S., Le Rouzic, V., Hunkele, A., Uprety, R., Huang, X.P., Xu, J., Roth, B.L., Pan, Y.X., Pasternak, G.W., 2018. Pharmacological characterization of novel synthetic opioids (NSO) found in the recreational drug marketplace. Neuropharmacology 134 (Pt A), 101–107. https://doi.org/10.1016/j.neuropharm.2017.08.016.

Besson, J.M., Besse, D., Lombard, M.C., 1992. Opioid peptides and pain regulation studied in animal models. Clin. Neuropharmacol. 15 (Suppl. 1 Pt A), 52a53a. https://doi.org/10.1097/00002826-199201001-00029.

Bilel, S., Azevedo, N.J., Arfè, R., Tirri, M., Gregori, A., Serpelloni, G., De-Giorgio, F., Frisoni, P., Neri, M., Calò, G., Marti, M., 2020 Jul. In vitro and in vivo pharmacological characterization of the synthetic opioid MT-45. Neuropharmacology 171, 108110. https://doi.org/10.1016/j.neuropharm.2020.108110. Epub 2020 Apr 25. PMID: 32344007.

Bilel, S., Tirri, M., Arfè, R., Sturaro, C., Fantinati, A., Cristofori, V., Bernardi, T., Boccuto, F., Cavallo, M., Cavalli, A., De-Giorgio, F., Calò, G., Marti, M., 2021. In vitro and in vivo pharmaco-toxicological characterization of 1-Cyclohexyl-x-methoxybenzene derivatives in mice: comparison with tramadol and PCP. Int. J. Mol. Sci. 22 (14), 7659. https://doi.org/10.3390/ijms22147659.

Blasco, T.A., Lee, D., Amalric, M., Swerdlow, N.R., Smith, N.T., Koob, G.F., 1986. The role of the nucleus raphe pontis and the caudate nucleus in alfentanil rigidity in the rat. Brain Res. Oct 29;386 (1–2), 280–286. https://doi.org/10.1016/0006-8993(86)90164-2.PMID:3096494.

Blauw, G.J., Westendorp, R.G., Simons, M., Chang, P.C., Frölich, M., Meinders, A.E., 1995. beta-Adrenergic receptors contribute to hypoxaemia induced vasodilation in man. Br. J. Clin. Pharmacol. 40 (5), 453–458.

Bohn, L.M., Lefkowitz, R.J., Gainetdinov, R.R., Peppel, K., Caron, M.G., Lin, F.T., 1999. Enhanced morphine analgesia in mice lacking beta-arrestin 2. Science (New York, N. Y.) 286 (5449), 2495–2498. https://doi.org/10.1126/science.286.5449.2495.

Bohn, L.M., Dykstra, L.A., Lefkowitz, R.J., Caron, M.G., Barak, L.S., 2004. Relative opioid efficacy is determined by the complements of the G protein-coupled receptor desensitization machinery. Mol. Pharmacol. 66 (1), 106–112. https://doi.org/10.1124/mol.66.1.106.

Camarda, V., Calo, G., 2013. Chimeric G proteins in fluorimetric calcium assays: experience with opioid receptors. Methods Mol. Biol. 937, 293–306. https://doi.org/10.1007/978-1-62703-086-1_18.

Canazza, I., Ossato, A., Trapella, C., Fantinati, A., De Luca, M.A., Margiani, G., Marti, M., 2016. Effect of the novel synthetic cannabinoids AKB48 and 5F-AKB48 on "tetrad", sensorimotor, neurological and neurochemical responses in mice. In vitro and in vivo pharmacological studies. Psychopharmacology (Berlin) 233 (21–22), 3685–3709. https://doi.org/10.1007/s00213-016-4402-y.

Chaillet, P., Marçais-Collado, H., Costentin, J., 1983 Nov 21. Catatonic or hypotonic immobility induced in mice by intracerebroventricular injection of mu or kappa opioid receptor agonists as well as enkephalins or inhibitors of their degradation. Life Sci. 33 (21), 2105–2111. https://doi.org/10.1016/0024-3205(83)90334-x.

Coopman, V., Cordonnier, J., De Leeuw, M., Cirimele, V., 2016. Ocfentanil overdose fatality in the recreational drug scene. Forensic Sci. Int. 266 (Suppl. C), 469–473. https://doi.org/10.1016/j.forsciint.2016.07.005.

Çoruh, B., Tonelli, M.R., Park, D.R., 2013 Apr. Fentanyl-induced chest wall rigidity. Chest 143 (4), 1145–1146. https://doi.org/10.1378/chest.12-2131.

DeWire, S.M., Yamashita, D.S., Rominger, D.H., Liu, G., Cowan, C.L., Graczyk, T.M., Chen, X.T., Pitis, P.M., Gotchev, D., Yuan, C., Koblish, M., Lark, M.W., Violin, J.D., 2013. A G protein-biased ligand at the μ-opioid receptor is potently analgesic with reduced gastrointestinal and respiratory dysfunction compared with morphine. J. Pharmacol. Exp. Therapeut. 344 (3), 708–717. https://doi.org/10.1124/jpet.112.201616.

Di Chiara, G., Imperato, A., 1988. Opposite effects of mu and kappa opiate agonists on dopamine release in the nucleus accumbens and in the dorsal caudate of freely moving rats. J. Pharmacol. Exp. Therapeut. 244 (3), 1067–1080.

Doshi, R., Majmundar, M., Kansara, T., et al., 2019. Frequency of cardiovascular events and in hospital mortality with opioid overdose hospitalizations. Am. J. Cardiol. 124, 1528–1533.

Eshleman, A.J., Nagarajan, S., Wolfrum, K.M., Reed, J.F., Nilsen, A., Torralva, R., Janowsky, A., 2020 Dec. Affinity, potency, efficacy, selectivity, and molecular modeling of substituted fentanyls at opioid receptors. Biochem. Pharmacol. 182, 114293. https://doi.org/10.1016/j.bcp.2020.114293. Epub 2020 Oct 20. PMID: 33091380.

Essawi, M.Y.H., 1998. Synthesis of fentanyl analogues as nonequilibrium irreversible ligands for opioid receptors. Bull Fac Pharmacy (Cairo Univ) 36 (3), 39–45.

Essawi, M.Y.H., 1999. Fentanyl analogues with a modified propanamido group as potential affinity labels: synthesis and in vivo activity. Pharmazie 54, 307.

Fantinati, A., Ossato, A., Bianco, S., Canazza, I., De Giorgio, F., Trapella, C., Marti, M., 2017. 1-cyclohexyl-x-methoxybenzene derivatives, novel psychoactive substances seized on the internet market. Synthesis and in vivo pharmacological studies in mice. Hum. Psychopharmacol. 32 (3) https://doi.org/10.1002/hup.2560.

Fletcher, J.E., Sebel, P.S., Murphy, M.R., Mick, S.A., Fein, S., 1991. Comparison of ocfentanil and fentanyl as supplements to general anesthesia. Anesth. Analg. 73, 622–626. https://doi.org/10.1213/00000539-199111000-00019.

Frisoni, P., Bacchio, E., Bilel, S., Talarico, A., Gaudio, R.M., Barbieri, M., et al., 2018. Novel synthetic opioids: the pathologist's point of view. Brain Sci. 8 (9) https://doi.org/10.3390/brainsci8090170.

Gill, H., Kelly, E., Henderson, G., 2019. How the complex pharmacology of the fentanyls contributes to their lethality. Addiction 114 (9), 1524–1525. https://doi.org/10.1111/add.14614.

Gillis, A., Gondin, A.B., Kliewer, A., Sanchez, J., Lim, H.D., Alamein, C., Manandhar, P., Santiago, M., Fritzwanker, S., Schmiedel, F., Katte, T.A., Reekie, T., Grimsey, N.L., Kassiou, M., Kellam, B., Krasel, C., Halls, M.L., Connor, M., Lane, J.R., Schulz, S., Canals, M., 2020 a. Low intrinsic efficacy for G protein activation can explain the improved side effect profiles of new opioid agonists. Sci. Signal. 13 (625) https://doi.org/10.1126/scisignal.aaz3140 eaaz3140.

Gillis, A., Kliewer, A., Kelly, E., Henderson, G., Christie, M.J., Schulz, S., Canals, M., 2020 b. Critical assessment of G protein-biased agonism at the μ-opioid receptor. Trends Pharmacol. Sci. 41 (12), 947–959. https://doi.org/10.1016/j.tips.2020.09.009.

Glaum, S.R., Miller, R.J., Hammond, D.L., 1994. Inhibitory actions of delta 1-, delta 2-, and mu-opioid receptor agonists on excitatory transmission in lamina II neurons of adult rat spinal cord. J. Neurosci. 14 (8), 4965–4971.

Gurtu, S., 1990. Mu receptor-serotonin link in opioid induced hyperactivity in mice. Life Sci. 46 (21), 1539–1544. https://doi.org/10.1016/0024-3205(90)90427-s.

Helander, A., Bradley, M., Hasselblad, A., Norlen, L., Vassilaki, I., Backberg, M., Lapins, J., 2017a. Acute skin and hair symptoms followed by severe, delayed eye complications in subjects using the synthetic opioid MT-45. Br. J. Dermatol. 176 (4), 1021–1027. https://doi.org/10.1111/bjd.15174.

Helander, A., Bäckberg, M., Signell, P., Beck, O., 2017 Jul. Intoxications involving acrylfentanyl and other novel designer fentanyls - results from the Swedish STRIDA project. Clin. Toxicol. 55 (6), 589–599. https://doi.org/10.1080/15563650.2017.1303141.

Hill, R., Santhakumar, R., Dewey, W., Kelly, E., Henderson, G., 2020 Jan. Fentanyl depression of respiration: comparison with heroin and morphine. Br. J. Pharmacol. 177 (2), 254–266. https://doi.org/10.1111/bph.14860. Epub 2019 Dec 23. PMID: 31499594; PMCID: PMC6989952.

Huang, B.-S., Terrell, R.C., Deutsche, K.H., Kudzma, L.V., Lalinde, N.L., 1986. N-aryl-N-(4-piperidinyl) Amides and Pharmaceutical Compositions and Method Employing Such Compounds. U.S. Patent, New Providence, NJ, p. 4584303A. Anaquest Inc.

Hustveit, O., 1994. Binding of fentanyl and pethidine to muscarinic receptors in rat brain. Jpn. J. Pharmacol. 64 (1), 57–59. https://doi.org/10.1254/jjp.64.57.

Kang, Yeona, Kelly, A., 24 January 2022. O'Conor, Andrew Kelleher et al. Naloxone's displacement of [11C]carfentanil and duration of receptor occupancy in the rat brain: implications. for opioid overdose reversal. https://doi.org/10.21203/rs.3.rs-1236438/v1. PREPRINT (Version 1) available at: Research Square.

Kenakin, T., 2004 Jan. Efficacy as a vector: the relative prevalence and paucity of inverse agonism. Mol. Pharmacol. 65 (1), 2–11. https://doi.org/10.1124/mol.65.1.2.PMID: 14722230.

Kitamura, S., Kawano, T., Kaminaga, S., Yamanaka, D., Tateiwa, H., Locatelli, F.M., Yokoyama, M., 2016. Effects of fentanyl on serotonin syndrome-like behaviors in rats. J. Anesth. 30 (1), 178–182. https://doi.org/10.1007/s00540-015-2092-y.

Klebacher, R., Harris, M.I., Ariyaprakai, N., Tagore, A., Robbins, V., Dudley, L.S., Bauter, R., Koneru, S., Hill, R.D., Wasserman, E., Shanes, A., Merlin, M.A., 2017. Incidence of naloxone redosing in the age of the new opioid epidemic. Prehosp. Emerg. Care: official journal of the National Association of EMS Physicians and the National Association of State EMS Directors 21 (6), 682–687. https://doi.org/10.1080/10903127.2017.1335818.

Kliewer, A., Schmiedel, F., Sianati, S., Bailey, A., Bateman, J.T., Levitt, E.S., Williams, J. T., Christie, M.J., Schulz, S., 2019 Jan 21. Phosphorylation-deficient G-protein-biased μ-opioid receptors improve analgesia and diminish tolerance but worsen opioid side effects. Nat. Commun. 10 (1), 367. https://doi.org/10.1038/s41467-018-08162-1.PMID:30664663;PMCID:PMC6341117.

Kliewer, A., Gillis, A., Hill, R., Schmiedel, F., Bailey, C., Kelly, E., Henderson, G., Christie, M.J., Schulz, S., 2020. Morphine-induced respiratory depression is independent of β-arrestin2 signalling. Br. J. Pharmacol. 177 (13), 2923–2931. https://doi.org/10.1111/bph.15004.

Krantz, M.J., Palmer, R.B., Haigney, M.C.P., 2021 Jan 19. Cardiovascular complications of opioid use: JACC state-of-the-art review. J. Am. Coll. Cardiol. 77 (2), 205–223. https://doi.org/10.1016/j.jacc.2020.11.002. PMID: 33446314.

Kuczyńska, K., Grzonkowski, P., Kacprzak, Ł., Zawilska, J.B., 2018. Abuse of fentanyl: an emerging problem to face. Forensic Sci. Int. 289, 207–214. https://doi.org/10.1016/j.forsciint.2018.05.042.

Lambert, D., Calo, G., 2020. Approval of oliceridine (TRV130) for intravenous use in moderate to severe pain in adults. Br. J. Anaesth. 125 (6), e473–e474. https://doi.org/10.1016/j.bja.2020.09.021.

Lazorthes, Y., Verdie, J.C., Caute, B., Maranhao, R., Tafani, M., 1988. Intracerebroventricular morphinotherapy for control of chronic cancer pain. Prog. Brain Res. 77, 395–405. https://doi.org/10.1016/s0079-6123(08)62804-6.

Le Bars, D., Gozariu, M., Cadden, S.W., 2001 Dec. Animal models of nociception. Pharmacol. Rev. 53 (4), 597–652. PMID: 11734620.

Lemmens, H.J., 1995. Pharmacokinetic-pharmacodynamic relationships for opioids in balanced anaesthesia. Clin. Pharmacokinet. 29 (4), 231–242. https://doi.org/10.2165/00003088-199529040 00003.

Lui, P.W., Lee, T.Y., Chan, S.H., 1989 Jan 2. Involvement of locus coeruleus and noradrenergic neurotransmission in fentanyl-induced muscular rigidity in the rat. Neurosci. Lett. 96 (1), 114–119. https://doi.org/10.1016/0304-3940(89)90252-8.PMID:2564649.

Malfacini, D., Ambrosio, C., Gro', M.C., Sbraccia, M., Trapella, C., Guerrini, R., et al., 2015. Pharmacological profile of nociceptin/orphanin FQ receptors interacting with G-proteins and b-arrestins 2. PLoS One 10, e132865. https://doi.org/10.1371/journal.pone.0132865.

Manglik, A., Lin, H., Aryal, D.K., McCorvy, J.D., Dengler, D., Corder, G., Levit, A., Kling, R.C., Bernat, V., Hübner, H., Huang, X.P., Sassano, M.F., Giguère, P.M., Löber, S., Duan, Da, Scherrer, G., Kobilka, B.K., Gmeiner, P., Roth, B.L., Shoichet, B. K., 2016. Structure-based discovery of opioid analgesics with reduced side effects. Nature 537 (7619), 185–190. https://doi.org/10.1038/nature19112.

Marti, M., Neri, M., Bilel, S., Di Paolo, M., La Russa, R., Ossato, A., Turillazzi, E., 2019. MDMA alone affects sensorimotor and prepulse inhibition responses in mice and rats: tips in the debate on potential MDMA unsafety in human activity. Forensic Toxicol. 37 (1), 132–144. https://doi.org/10.1007/s11419-018-0444-7.

Martin, D.C., Introna, R.P., Aronstam, R.S., 1991 Apr. Fentanyl and sufentanil inhibit agonist binding to 5-HT1A receptors in membranes from the rat brain.

Neuropharmacology 30 (4), 323–327. https://doi.org/10.1016/0028-3908(91)90056-h.PMID:1830134.
Matsui, A., Jarvie, B.C., Robinson, B.G., Hentges, S.T., Williams, J.T., 2014. Separate GABA afferents to dopamine neurons mediate acute action of opioids, development of tolerance, and expression of withdrawal. Neuron 82 (6), 1346–1356. https://doi.org/10.1016/j.neuron.2014.04.030.
Molinari P, Vezzi V, Sbraccia M, Grò C, Riitano D, Ambrosio C, Casella I, Costa T. Morphine-like opiates selectively antagonize receptor-arrestin interactions. J. Biol. Chem.. 2010 Apr 23;285(17):12522-12535. doi: 10.1074/jbc.M109.059410. Epub 2010 Feb 26. PMID: 20189994; PMCID: PMC2857100.
Nakamura, A., Yasufuku, K., Shimada, S., Aritomi, H., Furue, Y., Chiba, H., Muramoto, M., Takase, K., Koike, K., Matsumoto, T., Shimada, T., Watari, R., Matsuzaki, T., Asaki, T., Kanemasa, T., Fujita, M., 2020. The antagonistic activity profile of naloxone in μ-opioid receptor agonist-induced psychological dependence. Neurosci. Lett. 735, 135177. https://doi.org/10.1016/j.neulet.2020.135177.
Neubig, R.R., Spedding, M., Kenakin, T., Christopoulos, A., 2003. International union of pharmacology committee on receptor nomenclature and drug classification. XXXVIII. Update on terms and symbols in quantitative pharmacology. Pharmacol. Rev. 55, 597–606. https://doi.org/10.1124/pr.55.4.4.
Ossato, A., Vigolo, A., Trapella, C., Seri, C., Rimondo, C., Serpelloni, G., Marti, M., 2015. JWH-018 impairs sensorimotor functions in mice. Neuroscience 300, 174–188. https://doi.org/10.1016/j.neuroscience.2015.05.021.
Ossato, A., Canazza, I., Trapella, C., Vincenzi, F., De Luca, M.A., Rimondo, C., Marti, M., 2016. Effect of JWH-250, JWH-073 and their interaction on "tetrad", sensorimotor, neurological and neurochemical responses in mice. Prog. Neuro-Psychopharmacol. Biol. Psychiatry 67, 31–50. https://doi.org/10.1016/j.pnpbp.2016.01.007.
Ossato, A., Bilel, S., Gregori, A., Talarico, A., Trapella, C., Gaudio, R.M., et al., 2018. Neurological, sensorimotor and cardiorespiratory alterations induced by methoxetamine, ketamine and phencyclidine in mice. Neuropharmacology 141, 167–180. https://doi.org/10.1016/j.neuropharm.2018.08.017.
Pesavento, S., Bilel, S., Murari, M., Gottardo, R., Arfè, R., Tirri, M., Panato, A., Tagliaro, F., Marti, M., 2022. Zebrafish Larvae: A New Model to Study Behavioural Effects and Metabolism of Fentanyl, in Comparison to a Traditional Mice Model. Medicine, Science, and the Law. Advance online publication, 258024221074568. https://doi.org/10.1177/00258024221074568.
Raehal, K.M., Bohn, L.M., 2011. The role of beta-arrestin2 in the severity of antinociceptive tolerance and physical dependence induced by different opioid pain therapeutics. Neuropharmacology 60 (1), 58–65. https://doi.org/10.1016/j.neuropharm.2010.08.003.
Raehal, K.M., Walker, J.K., Bohn, L.M., 2005. Morphine side effects in beta-arrestin 2 knockout mice. J. Pharmacol. Exp. Therapeut. 314 (3), 1195–1201. https://doi.org/10.1124/jpet.105.087254.
Rodriguez-Arias, M., Broseta, I., Aguilar, M.A., Minarro, J., 2000. Lack of specific effects of selective D(1) and D(2) dopamine antagonists vs. risperidone on morphine-induced hyperactivity. Pharmacol. Biochem. Behav. 66 (1), 189–197. https://doi.org/10.1016/s0091-3057(00)00207-0.
Rzasa Lynn, R., Galinkin, J.L., 2018 Jan. Naloxone dosage for opioid reversal: current evidence and clinical implications. Ther Adv Drug Saf 9 (1), 63–88. https://doi.org/10.1177/2042098617744161.Epub.2017.Dec.13.PMID:29318006;PMCID:PMC5753997.
Sakai, M., Fukuyama, H., Sato, K., Kudoh, I., 2002. Masui. [Effects of fentanyl on acetylcholine release from hippocampus and righting reflex in rat: an in vivo brain microdialysis study]. Jpn. J. Anesthesiol. 51 (2), 118–123.
Schmid, C.L., Kennedy, N.M., Ross, N.C., Lovell, K.M., Yue, Z., Morgenweck, J., Cameron, M.D., Bannister, T.D., Bohn, L.M., 2017. Bias factor and therapeutic window correlate to predict safer opioid analgesics. Cell 171 (5), 1165–1175. https://doi.org/10.1016/j.cell.2017.10.035 e13.
Shi, Q., Li, M., Mika, D., Fu, Q., Kim, S., Phan, J., Shen, A., Vandecasteele, G., Xiang, Y.K., 2017. Heterologous desensitization of cardiac β-adrenergic signal via hormone-induced βAR/arrestin/PDE4 complexes. Cardiovasc. Res. 113 (6), 656–670. https://doi.org/10.1093/cvr/cvx036.
Soares, J.H., Brosnan, R.J., Smith, A., Mayhew, P.D., 2014. Rabbit model of chest wall rigidity induced by fentanyl and the effects of apomorphine. Respir. Physiol. Neurobiol. 202, 50–52. https://doi.org/10.1016/j.resp.2014.07.017.
Sohn, J.T., Ok, S.H., Kim, H.J., Moon, S.H., Shin, I.W., Lee, H.K., Chung, Y.K., 2004. Inhibitory effect of fentanyl on acetylcholine-induced relaxation in rat aorta. Anesthesiology 101 (1), 89–96. https://doi.org/10.1097/00000542-200407000-00015.
Solimini, R., Pichini, S., Pacifici, R., Busardò, F.P., Giorgetti, R., 2018 Jun 20. Pharmacotoxicology of non-fentanyl derived new synthetic opioids. Front. Pharmacol. 9, 654. https://doi.org/10.3389/fphar.2018.00654.PMID:29973882;PMCID:PMC6020781.
Somerville, N.J., O'Donnell, J., Gladden, R.M., Zibbell, J.E., Green, T.C., Younkin, M., Ruiz, S., Babakhanlou-Chase, H., Chan, M., Callis, B.P., Kuramoto-Crawford, J., Nields, H.M., Walley, A.Y., 2017 Apr 14. Characteristics of fentanyl overdose - Massachusetts, 2014-2016. MMWR Morb. Mortal. Wkly. Rep. 66 (14), 382–386. https://doi.org/10.15585/mmwr.mm6614a2.PMID:28406883;PMCID:PMC5657806.
Stein, C., Schafer, M., Machelska, H., 2003. Attacking pain at its source: new perspectives on opioids. Nat. Med. 9 (8), 1003–1008. https://doi.org/10.1038/nm908.
Torralva, R., Janowsky, A., 2019. Noradrenergic mechanisms in fentanyl-mediated rapid death explain failure of naloxone in the opioid crisis. J. Pharmacol. Exp. Therapeut. 371 (2), 453–475. https://doi.org/10.1124/jpet.119.258566.
Torralva, R., Eshleman, A.J., Swanson, T.L., Schmachtenberg, J.L., Schutzer, W.E., Bloom, S.H., Wolfrum, K.M., Reed, J.F., Janowsky, A., 2020. Fentanyl but not morphine interacts with nonopioid recombinant human neurotransmitter receptors and transporters. J. Pharmacol. Exp. Therapeut. 374 (3), 376–391. https://doi.org/10.1124/jpet.120.265561.
Torrecilla, M., Marker, C.L., Cintora, S.C., Stoffel, M., Williams, J.T., Wickman, K., 2002. G-protein-gated potassium channels containing Kir3.2 and Kir3.3 subunits mediate the acute inhibitory effects of opioids on locus ceruleus neurons. J. Neurosci. 22 (11), 4328–4334, 20026414.
United Nations Office on Drugs and Crime (UNDOC), 2020. World Drug Rapport. UNDOC.
Vandeputte, M.M., Cannaert, A., Stove, C.P., 2020. In vitro functional characterization of a panel of non-fentanyl opioid new psychoactive substances. Arch. Toxicol. 94 (11), 3819–3830. https://doi.org/10.1007/s00204-020-02855-7.
Vankova, M.E., Weinger, M.B., Chen, D.Y., Bronson, J.B., Motis, V., Koob, G.F., 1996 Sep. Role of central mu, delta-1, and kappa-1 opioid receptors in opioid-induced muscle rigidity in the rat. Anesthesiology 85 (3), 574–583. https://doi.org/10.1097/00000542-199609000-00017.PMID:8853088.
Varshneya, N.B., Walentiny, D.M., Moisa, L.T., Walker, T.D., Akinfiresoye, L.R., Beardsley, P.M., 2019 Jun. Opioid-like antinociceptive and locomotor effects of emerging fentanyl-related substances. Neuropharmacology 151, 171–179. https://doi.org/10.1016/j.neuropharm.2019.03.023. Epub 2019 Mar 20. PMID: 30904478.
Varshneya, N.B., Hassanien, S.H., Holt, M.C., Stevens, D.L., Layle, N.K., Bassman, J.R., Iula, D.M., Beardsley, P.M., 2022. Respiratory depressant effects of fentanyl analogs are opioid receptor-mediated. Biochem. Pharmacol. 195, 114805. https://doi.org/10.1016/j.bcp.2021.114805.
Vigolo, A., Ossato, A., Trapella, C., Vincenzi, F., Rimondo, C., Seri, C., Marti, M., 2015. Novel halogenated derivates of JWH-018: behavioral and binding studies in mice. Neuropharmacology 95, 68–82. https://doi.org/10.1016/j.neuropharm.2015.02.008.
Walker, E.A., Chambers, C., Korber, M.G., Tella, S.R., Prioleau, C., Fang, L., 2021. Antinociceptive and discriminative stimulus effects of six novel psychoactive opioid substances in male rats. J. Pharmacol. Exp. Therapeut. 379 (1), 1–11. https://doi.org/10.1124/jpet.121.000689.
Wall, P.D., 1967. The laminar organization of dorsal horn and effects of descending impulses. J. Physiol. 188 (3), 403–423. https://doi.org/10.1113/jphysiol.1967.sp008146.
Watanabe, S., Vikingsson, S., Roman, M., Green, H., Kronstrand, R., Wohlfarth, A., 2017 Jul. In vitro and in vivo metabolite identification studies for the new synthetic opioids Acetylfentanyl, acrylfentanyl, Furanylfentanyl, and 4-Fluoro-Isobutyrylfentanyl. AAPS J. 19 (4), 1102–1122. https://doi.org/10.1208/s12248-017-0070-z.Epub.2017.Apr.5.PMID:28382544.
Weinger, M.B., Cline, E.J., Smith, N.T., Blasco, T.A., Koob, G.F., 1988. Localization of brainstem sites which mediate alfentanil-induced muscle rigidity in the rat. Pharmacol. Biochem. Behav. 29, 573–580.
Wilde, M., Pichini, S., Pacifici, R., Tagliabracci, A., Busardò, F.P., Auwärter, V., Solimini, R., 2019 Apr 5. Metabolic pathways and potencies of new fentanyl analogs. Front. Pharmacol. 10, 238. https://doi.org/10.3389/fphar.2019.00238.PMID:31024296;PMCID:PMC6461066.
Yadav, S.K., Kumar, D., Kumar, P., Gupta, P.K., Bhattacharya, R., 2018 Jan/Feb. Biochemical, oxidative, and physiological changes caused by acute exposure of fentanyl and its 3 analogs in rodents. Int. J. Toxicol. 37 (1), 28–37. https://doi.org/10.1177/1091581817750560.Epub.2018.Jan.22. PMID: 29356587.
Yassen, A., Olofsen, E., Romberg, R., Sarton, E., Teppema, L., Danhof, M., Dahan, A., 2007. Mechanism-based PK/PD modeling of the respiratory depressant effect of buprenorphine and fentanyl in healthy volunteers. Clin. Pharmacol. Ther. 81 (1), 50–58. https://doi.org/10.1038/sj.clpt.6100025.
Zawilska, J.B., 2017 Jun 30. An expanding world of novel psychoactive substances: opioids. Front. Psychiatr. 8, 110. https://doi.org/10.3389/fpsyt.2017.00110.PMID:28713291;PMCID:PMC5492455.
Zhu, Y., Ge, B., Fang, S., Zhu, Y., Dai, Q., Tan, Z., Huang, Z., Ghen, X., 1981. Studies on potent analgesics. I. Synthesis and analgesic activity of derivatives of fentanyl (in Chinese). Yaoxue Xuebao [Acta Pharmaceutica Sinica 16, 199–210.
Zollner, C., Shaqura, M.A., Bopaiah, C.P., Mousa, S., Stein, C., Schafer, M., 2003. Painful inflammation-induced increase in mu-opioid receptor binding and G-protein coupling in primary afferent neurons. Mol. Pharmacol. 64 (2), 202–210. https://doi.org/10.1124/mol.64.2.202.